Arteriosclerosis, Thrombosis, and Vascular Biology

BASIC SCIENCES

PGC1α Regulates the Endothelial Response to Fluid Shear Stress via Telomerase Reverse Transcriptase Control of Heme Oxygenase-1

Shashi Kant[©], Khanh-Van Tran, Miroslava Kvandova[©], Amada D. Caliz, Hyung-Jin Yoo[©], Heather Learnard[©], Ana C. Dolan, Siobhan M. Craige, Joshua D. Hall[©], Juan M. Jiménez[©], Cynthia St. Hilaire[©], Eberhard Schulz, Swenja Kröller-Schön, John F. Keaney Jr[©]

OBJECTIVE: Fluid shear stress (FSS) is known to mediate multiple phenotypic changes in the endothelium. Laminar FSS (undisturbed flow) is known to promote endothelial alignment to flow, which is key to stabilizing the endothelium and rendering it resistant to atherosclerosis and thrombosis. The molecular pathways responsible for endothelial responses to FSS are only partially understood. In this study, we determine the role of PGC1 α (peroxisome proliferator gamma coactivator-1 α)-TERT (telomerase reverse transcriptase)-HMOX1 (heme oxygenase-1) during shear stress in vitro and in vivo.

APPROACH AND RESULTS: Here, we have identified PGC1 α as a flow-responsive gene required for endothelial flow alignment in vitro and in vivo. Compared with oscillatory FSS (disturbed flow) or static conditions, laminar FSS (undisturbed flow) showed increased PGC1 α expression and its transcriptional coactivation. PGC1 α was required for laminar FSS-induced expression of TERT in vitro and in vivo via its association with ERR α (estrogen-related receptor alpha) and KLF (Kruppel-like factor)-4 on the *TERT* promoter. We found that TERT inhibition attenuated endothelial flow alignment, elongation, and nuclear polarization in response to laminar FSS in vitro and in vivo. Among the flow-responsive genes sensitive to TERT status, HMOX1 was required for endothelial alignment to laminar FSS.

CONCLUSIONS: These data suggest an important role for a PGC1 α -TERT-HMOX1 axis in the endothelial stabilization response to laminar FSS.

GRAPHIC ABSTRACT: A graphic abstract is available for this article.

Key Words: atherosclerosis ■ heme oxygenase-1 ■ peroxisome proliferators ■ telomerase ■ thrombosis

ne endothelium exerts considerable control over vascular homeostasis with important roles governing vascular tone, inflammation, and metabolism. Normal endothelial function is characterized by a quiescent cell phenotype that is nonproliferative, nonmigratory, and exhibits a cell surface that prevents thrombosis, inflammation, and lipid deposition, thereby resisting atherosclerosis and vascular disease. A key stabilizing stimulus for endothelial quiescence is laminar fluid shear stress (FSS; also called undisturbed flow) passing over the cell surface—a common feature of straight vascular segments with little-to-no curvature. Endothelial cells reorient and change their shape to

align their long axis to physiological FSS.⁶ In contrast, curved and branched arteries experience multidirectional and chaotic FSS (also called disturbed flow). Areas with disturbed flow promote a less stable, activated, and dysfunctional endothelial phenotype that is more susceptible to inflammation and atherosclerosis.^{5,7–11} Thus, endothelial response to FSS is a critical element of vascular homeostasis.

Endothelial cell responses to FSS involve both mechanotransduction of the flow signal and coordinated regulation of signaling pathways and gene expression that dictate the phenotypic consequences. A number of mechanosensors and mechanotransducers have

Correspondence to: Shashi Kant, PhD, Harvard Medical School, Boston, MA. Email skant1@bwh.harvard.edu *S. Kant, K.-V. Tran, and M. Kvandova contributed equally.

Supplemental Material is available at https://www.ahajournals.org/doi/suppl/10.1161/ATVBAHA.121.317066.

For Sources of Funding and Disclosures, see page 32.

© 2021 American Heart Association, Inc.

Arterioscler Thromb Vasc Biol is available at www.ahajournals.org/journal/atvb

Nonstandard Abbreviations and Acronyms

ARE antioxidant response element **eNOS** endothelial NO synthase $ERR\alpha$ estrogen-related receptor alpha **FSS** fluid shear stress **HAEC** human aortic endothelial cell HMOX1 heme oxygenase-1 **HRP** horseradish peroxidase **KLF** Kruppel-like factor **MLEC** mouse lung endothelial cell PGC1α peroxisome proliferator gamma coactivator-1a **PGC1**α-**ECKO** endothelial knockout PGC-1 α **PGC1** α -**ECTG** endothelial-specific PGC1 α transgenic mice ROS reactive oxygen species SCG single-copy gene **TERT** telomerase reverse transcriptase

been implicated in flow sensing, including ion channels, PECAM-1 (platelet endothelial cell adhesion molecule-1), G-protein-coupled receptors, junctional proteins, VEGF (vascular endothelial growth factor) receptors, and even primary cilia.57,712,13 Several pathways have been implicated in the phenotypic response to physiological versus pathological flow. For example, disturbed flow enhances NF-κB (nuclear factor kappa B), Yap/Taz, β-catenin, and the SMAD2/3 (mothers against decapentaplegic homolog 2/3) pathways that cooperate to promote remodeling that includes activation of inflammatory mediators and, perhaps, induction of endothelial-to-mesenchymal transition. 14-16 In contrast, laminar flow leads to activation of the KLF (Kruppel-like factor)-2/4, Notch, and ALK1 (activin receptor-like kinase 1)-SMAD1/5 pathways that induce genes required for vascular stability. 17-19 In particular, KLF2 and KLF4 have been implicated in promoting vasodilation and the inhibition of both inflammation and thrombosis.20 Among the genes regulated by KLF2 and KLF4, NOS3 codes for eNOS (endothelial NO synthase).20 This enzyme contributes importantly to the vascular homeostatic environment by promoting vasodilation and limiting atherothrombosis. We recently reported that the transcriptional coactivator PGC1 α (peroxisome proliferator gamma coactivator-1α) was an important determinant of eNOS expression in vitro and in vivo.21 Here we sought to determine whether PGC1 α and its downstream targets play a role in endothelial responses to FSS.

MATERIALS AND METHODS

The data that support the findings of this study are available from the corresponding author upon reasonable request.

Highlights

- PGC-1α (peroxisome proliferator coactivator-1α) is a flow-responsive gene required for laminar flow-induced endothelial cell alignment in vitro and in vivo.
- PGC-1 α regulates laminar fluid shear stressinduced expression of TERT (telomerase reverse transcriptase) in vitro and in vivo.
- PGC1 α forms a complex with ERR α (estrogenrelated receptor alpha) and KLF (Kruppel-like factor)-4 on the TERT promoter.
- PGC1 α -TERT axis is vital for expression of HMOX1 (heme oxygenase-1)-a gene required for endothelial alignment during laminar fluid shear stress.

Animals

C57BL/6J, Tie2-Cre (#008863), and VE-Cadherin-Cre (#006137) strains of mice were obtained from The Jackson Laboratory. PGC1 α transgenic mice, ²¹ conditional PGC1 α , ²² TERT (telomerase reverse transcriptase) global knockout,23 and conditional TERT²⁴ mice were described previously. For the creation of endothelial knockout lines, conditional PGC-1α allele (LoxP sites flanking exons 3-5-a kind gift from Dr Bruce Spiegelman, Harvard University)²² or TERT allele (LoxP sites flanking exons 1-2) mice were crossed with either VE-cadherin-Cre or Tie2-Cre mouse lines on the C57BL/6J background. These endothelial knockout PGC-1α (PGC1α-ECKO) or TERT-ECKO mice were compared with Cre control mice. Endothelial-specific PGC1lphatransgenic mice (PGC1α-ECTG) were produced with human PGC-1 α expression under the control of the mouse vascular endothelial cadherin promoter (VE-Cadherin) as described.21

All mouse experiments were performed according to the relevant ethical regulations. Mice were housed in facilities either accredited by the American Association for Laboratory Animal Care or approved by the Ethics Committee of the University Hospital Mainz and Landesuntersuchungsamt Koblenz (23 177-07/G 12-1-080 and 23 177-07/G 17-1-066). Animal protocols were approved by the Institutional Animal Care and Use Committee of the Brigham and Women's Hospital, Boston.

Voluntary Exercise in Mice

Exercise experiments were performed with 4-week-old animals that were kept in individual cages for 6 weeks equipped with a running wheel and a mileage counter. Exercise training was performed voluntarily. The running distance of Tie2Cre control and PGC1 α -ECKO mice did not differ significantly.

Cell Culture

Human aortic endothelial cells (HAECs; #PCS-100-011) and human umbilical vein endothelial cells (#PCS100010) were purchased from ATCC and cultured in endothelial cell growth basal medium-2 containing bullet kit growth factor supplements (EBM-2 [endothelial cell growth basal medium-2]; Lonza), 5% fetal bovine serum, 100 units/mL penicillin, 100 µg/mL streptomycin, and 2 mmol/L L-glutamine (Invitrogen). Cultured human ECs between passages 2 and 6 were utilized for experiments.

Adult mice were sacrificed for lung endothelial cell (mouse lung endothelial cell [MLEC]) isolation according to approved guidelines as mentioned above. Pooled mouse lungs were immediately harvested and minced. Tissues were then transferred to a fresh conical tube containing digestion solution, 50 mg/mL type 1 filtered collagenase (Worthington) in DMEM media, and incubated at 37 °C for 1 hour. The enzyme digested tissue was filtered through 70- and 40- μ m cell strainers. The cell suspension was pelleted by centrifugation at 300g for 10 minutes at room temperature. The isolated cells were further used for sorting and direct mRNA isolation or for cell culture experiments. 25

For direct use of the cells in RT-qPCR (real-time quantitative polymerase chain reaction) measurements, 2 separation steps were performed to isolate endothelial cells using CD31 (cluster of differentiation 31) MACS (CD31 Micro Beads mouse, 130-097-418; Miltenyi Biotech) and ICAM (intercellular adhesion molecule) Dynabeads (rat anti-mouse CD102/ICAM2, 553326; BD Bioscience) according to the manufacturer's protocols. For cell culture experiments, pellets were resuspended in MLEC growth media containing a 1:1 mixture of DMEM and Ham's F-12 (Gibco), 20% fetal bovine serum, 50 mg endothelial mitogen (Cell Applications), 50 mg/mL heparin (Sigma), 100 units/mL penicillin, and 100 µg/mL streptomycin and plated on 0.2% gelatin-coated cell flasks. Media was changed daily. At 80% confluency, cells were collected in a conical tube with 25 µL Dynabeads sheep anti-Rat IgG (Invitrogen) coated with ICAM-2 (BD Biosciences Pharmingen) for the first selection. The cell-Dynabead suspension was set to rotate at 4°C for 40 minutes and harvested on a magnetic rack. The beads were resuspended in MLEC growth medium and plated into a new 0.2% gelatin-coated cell flask. When cells reached 80% confluency, the above steps were repeated for the second selection. MLEC used for experiments were between passages 2 and 4. Preliminary experiments did not reveal any effect of sex on in vitro cell culture experiments consistent with prior experience.²⁵ Therefore, cell culture work here generally involved pooled cells isolated from 2 to 3 mice regardless of sex except in Figure 1 MLECs were from male mice and data in Figures 3 and 6 were derived from female MLECs.

Adenoviral Constructs

Downloaded from http://ahajournals.org by on July 14, 2022

Adenoviral vectors were used for both overexpression (24 hours) and knockdown (48 hours) of PGC1 α . The PGC1 α expressing vector was a kind gift from Dr Bruce Spiegelman, Harvard University, and the ERR α (estrogen-related receptor alpha) vector was a kind gift from Dr Anastasia Kralli, Scripps Research Institute. Control viruses (siCtl, LacZ, and GFP) from Vector BioLabs (Malvern, PA) were used for comparison. Cells were typically infected at a multiplicity of infection of 10 to 50 with a control adenovirus at the same multiplicity of infection.

Transfections

Transfection assays were performed using 100-nM small interfering human RNA oligonucleotides (ON-TARGET plus SMART pool; Horizon Discovery Dharmacon, Lafayette, CO) for control (D-001810-10), *TERT* (L-003547-00), *KLF4* (L-005089-00), *ERRα* (L-003403-00), and *HMOX1* (heme oxygenase-1; L-006372-00) in DharmaFECT 3 reagent (T-2003; Horizon Discovery Dharmacon) for 6 hours in OptiMEM (Invitrogen, Waltham, MA).²⁷ Media was then changed to EBM-2 growth medium. For flow experiments, after 48 hours of siRNA treatment,

cells were exposed to either laminar flow 12 dynes/cm² or oscillatory flow of 4 dynes/cm² (Ibidi System) for 48 hours.

Total RNA Preparation and Quantitative Polymerase Chain Reaction

Cell and tissues were lysed with TRIzol reagent (Life Science Technologies), and total RNA was extracted using the RNeasy Plus Micro Kit (Qiagen). Total RNA was reverse transcribed with oligo (dT) primers for cDNA synthesis using an iScript cDNA synthesis kit (Bio-Rad). The expression of mRNA was examined by quantitative PCR analysis using a QuantStudio 6 Flex Real-Time PCR System (Applied Biosystems). TaqMan assays were used to quantitate.

ERRα (Hs00607062_gH), HEY1 (Hs05047713_s1, Mm00 468865_m1), HMOX1 (Hs01110250_m1, Mm00516005_ m1), ICAM1 (Mm00516023_m1Hs00164932_m1), KLF2 (Hs00360439_g1, Mm00500486_g1), KLF4 (Hs003588 36_m1, Mm00516104_m1), $PGC1\alpha$ (Hs01016719_m1, Hs01016724_m1, Mm01208835_m1), TERT (Mm01352136_ m1), VCAM1 (Mm01320970_m1, Hs01003372_m1), MMP2 (matrix metallopeptidase 2; Mm00439498_m1), ATXN1 (ataxin-1)/Sca1 (spinocerebellar ataxia type 1; Mm00485928_ m1), SM22α (smooth muscle protein 22-alpha)/TAGLN Mm00441660_m1), (transgelin; TBP (Mm00446973_ **HPRT** (Hs02800695_m1, Mm00446968_m1), m1), GAPDH (Hs99999905_m1, 4352339E-0904021), B2M (Hs9999907_m1, Mm00437762_m1) mRNA (Applied Biosystems). The $2^{-\Delta\Delta CT}$ method was used for relative quantification of gene expression. 28,29 Expression of HPRT, GAPDH, TBP, and B2M was used to normalize each sample.

Immunoblot Analysis

Cell extracts were prepared using Triton lysis buffer (TLB buffer; 20 mmol/L Tris [pH 7.4], 1% Triton X-100, 10% glycerol, 137 mmol/L NaCl, 2 mmol/L EDTA, 25 mmol/L β-glycerophosphate) with proteinase inhibitors (Sigma #11873580001) and phosphatase inhibitors (Sigma #4906837001).³⁰ Protein extracts (50 μg) in β-mercaptoethanol containing SDS sample buffer were separated in 4% to 12% gradient SDS-polyacrylamide gels (#456-8094; Bio-Rad), transferred to nitrocellulose membranes (#170-4271; Bio-Rad, Hercules, CA) and incubated with primary antibody at 1:1000 dilution. Immunocomplexes were visualized with HRP (horseradish peroxidase)-conjugated secondary antibodies and detected with a Clarity Western ECL substrate (#170-5061; Bio-Rad, Hercules, CA). Images were acquired on a chemiluminescent imager (Bio-Rad Chem-Doc Imaging System).

Antibodies and Reagents

Primary antibodies for immunoblots were obtained from Abcam (HMOX1 #52947, TERT #ab32020, Cambridge, MA), Cell Signaling (ERR α #13826, Danvers, MA), R&D (KLF4 #AF3640), Novus Bio (PGC1 α #NBP-04676, Centennial, CO), BD Pharmingen (CD31 #550274, San Jose, CA), and Sigma (β -catenin, #C2206, St. Louis, MO). Control antibodies were obtained from Proteintech (GAPDH #HRP-60004 and β -actin #HRP-60008, Rosemont, IL). The TERT inhibitor BIBR1532 was purchased from Selleck Chemicals (Houston, TX). The HMOX1 inhibitor, zinc (II) protoporphyrin IX and control, copper protoporphyrin IX were purchased from Sigma. The

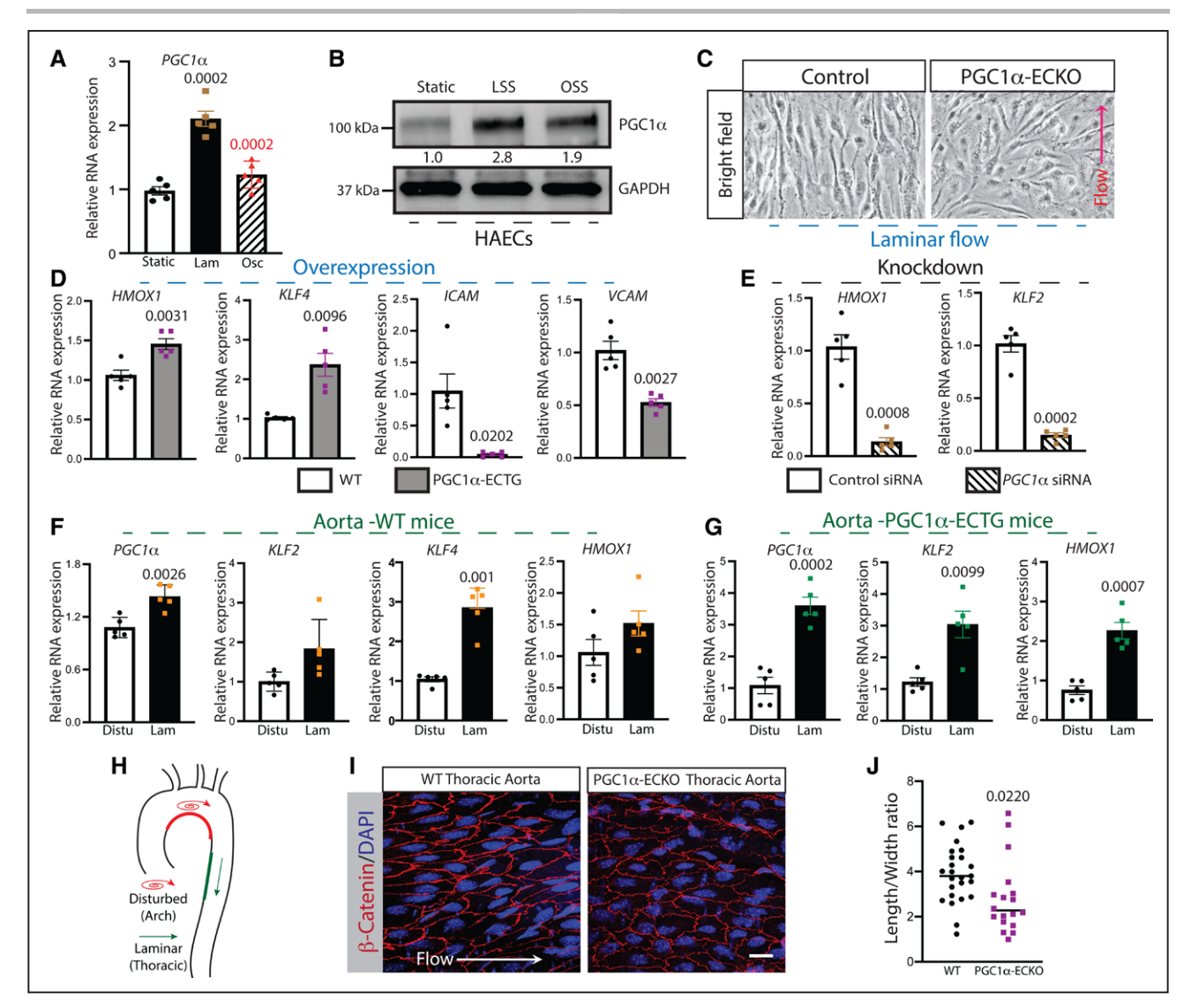


Figure 1. PGC1α (peroxisome proliferator gamma coactivator-1α) regulates endothelial cell function during fluid shear stress. A and B, PGC1 a mRNA expression (A) or protein expression (B) from human aortic endothelial cells (HAECs) was measured by RT-qPCR (real-time quantitative polymerase chain reaction) or Western blots after cells were subjected to static, laminar, or oscillatory fluid shear stress (FSS) for 48 h (n=5). C, Bright-field image of mouse lung endothelial cells (MLECs) isolated from either WT (wild type) or PGC1α-ECKO mice after exposure to laminar FSS. D, MLECs from WT and PGC1α-ECTG mice were exposed to laminar FSS, and RT-qPCR was performed for the indicated genes (n=5). E, HAECs were treated with scrambled or PGC1α siRNA, and RT-qPCR was performed for the indicated genes after exposure to laminar FSS for 48 h (n=5). F and G, Aortae were isolated from either WT (F) or PGC1α-ECTG (G) mice, mRNA isolated, and RT-qPCR performed in the indicated regions reflecting disturbed or laminar flow (n=5). H, Sample sites of disturbed (oscillatory) vs laminar fluid shear stress in mouse aorta. I, En face staining with β-catenin and DAPI in WT and PGC1α-ECKO aorta. Scale bar, 20 μm. J, Composite data of length/width ratio of the endothelium in the thoracic region of mouse aortae (n=18-24). All experiments were repeated 3 to 5x. Statistically significant differences were measured by Student t test or 1-way ANOVA with post hoc comparison as appropriate with control group. The data are mean±SEM.

HMOX1 inhibitor 1-[[2-[2-(4-bromophenyl)ethyl]-1,3-dioxolan-2-yl]methyl]-1*H*- imidazole hydrochloride (OB 24 hydrochloride) was purchased from Tocris Bioscience (Minneapolis, MN).

Immunoprecipitation

Cell extracts were prepared using Triton lysis buffer and incubated (16 hours, 4°C) with either 3 µg nonimmune control rabbit IgG (Cell Signaling #2729) or with the ERRa antibody (Cell Signaling #13826) to 500 uL of cell lysate. Immunocomplexes were isolated using Protein G Sepharose beads (Santa Cruz #SC2002, Santa Cruz, CA) and washed 4 to 5× with lysis buffer. Bead pellets were resuspended and boiled in β-mercaptoethanol containing Laemmli sample buffer, separated in 4% to 12% gradient

SDS-polyacrylamide gels (Bio-Rad #456-8094), transferred to nitrocellulose membranes (Bio-Rad #170-4271, Hercules, CA) and incubated with rabbit anti PGC1 antibody with 1:1000 dilution. Immunocomplexes were visualized with HRP-conjugated goat anti-rabbit IgG (Cell Signaling, #7074) and detected with a Clarity Western ECL substrate (Bio-Rad #170-5061).

Chromatin Immunoprecipitation

Cultured HAECs were exposed to 1% oxygen for 30 minutes at 37°C and processed using a ChIP-IT kit (Active Motif #53008, Carlsbad, CA) according to the manufacturer's instructions. Briefly, the cells were fixed in 1% formalin and homogenized in lysis buffer. Lysed cells were sheared with sonication 10×

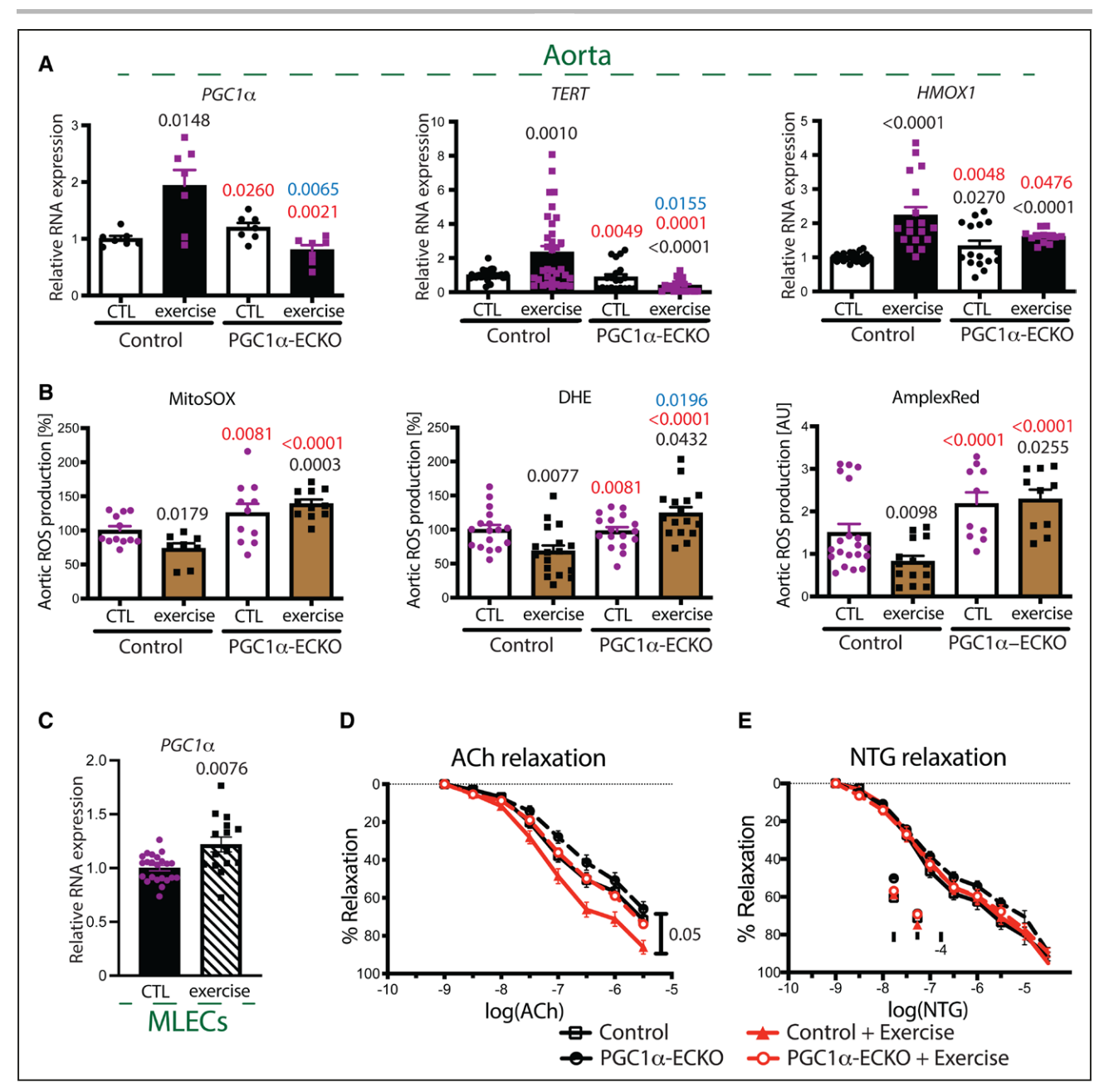


Figure 2. PGC1 α (peroxisome proliferator gamma coactivator-1 α) is required for endothelial functional responses to exercise. **A**, Aortae were isolated from WT (wild type) or PGC1 α -ECKO mice and gene expression determined in total aortic tissue by RT-qPCR (real-time quantitative polymerase chain reaction) for the indicated genes before and after exercise; n=7/group (PGC1 α mRNA expression), n=18-32/group (TERT [telomerase reverse transcriptase]), and n=12-21/group (HMOX1). **B**, Reactive oxygen species (ROS) production was measured as indicated in WT and PGC1 α -ECKO mice before and after exercise; n=8-12/group (MitoSOX), n=16-17/group (DHE), and n=10-20/group (AmplexRed). **C**, MLECs were isolated from WT mice with or without exercise and PGC1 α mRNA expression determined by RT-qPCR before and after exercise. **D**, Endothelial function measured as aortic isometric force in response to acetylcholine (Ach; n=10-12). **E**, Nitroglycerin-mediated smooth muscle cell function by treatment and genotype (NTG; n=8-12). Statistically significant differences were measured by Student *t* test or either 1- or 2-way ANOVA with post hoc comparison as appropriate with control group. The data are mean±SEM. *P* vs control mice (black); vs control + exercise mice (red) and vs PGC1 α -ECKO mice (blue).

each with a pulse of 20 seconds and 30 seconds of rest on ice between shearing steps. Sheared samples were incubated with Protein G Beads and either nonimmune IgG (Sigma #NI01), Polymerase II (Santa Cruz #sc56767) or PGC1 α (Novus Bio #NBP-04676, Centennial, CO) antibodies on an end-to-end rotator overnight at 4 °C. The beads binding target chromatin were washed on a magnetic bar with washing buffer. Elucidated chromatin targets were amplified with quantitative PCR using

a primer pair (5'-CAGAAGTTTCTCGCCCCCTT-3' and 5'-GAGGCCAACATCTGGTCAC-3') specific for the *TERT* promoter.

Whole Mount Aorta En Face Immunofluorescence Staining

Before excision, aortae were perfused serially via the left ventricle of the heart with (1) 0.5 mmol/L EDTA in PBS; (2) 4%

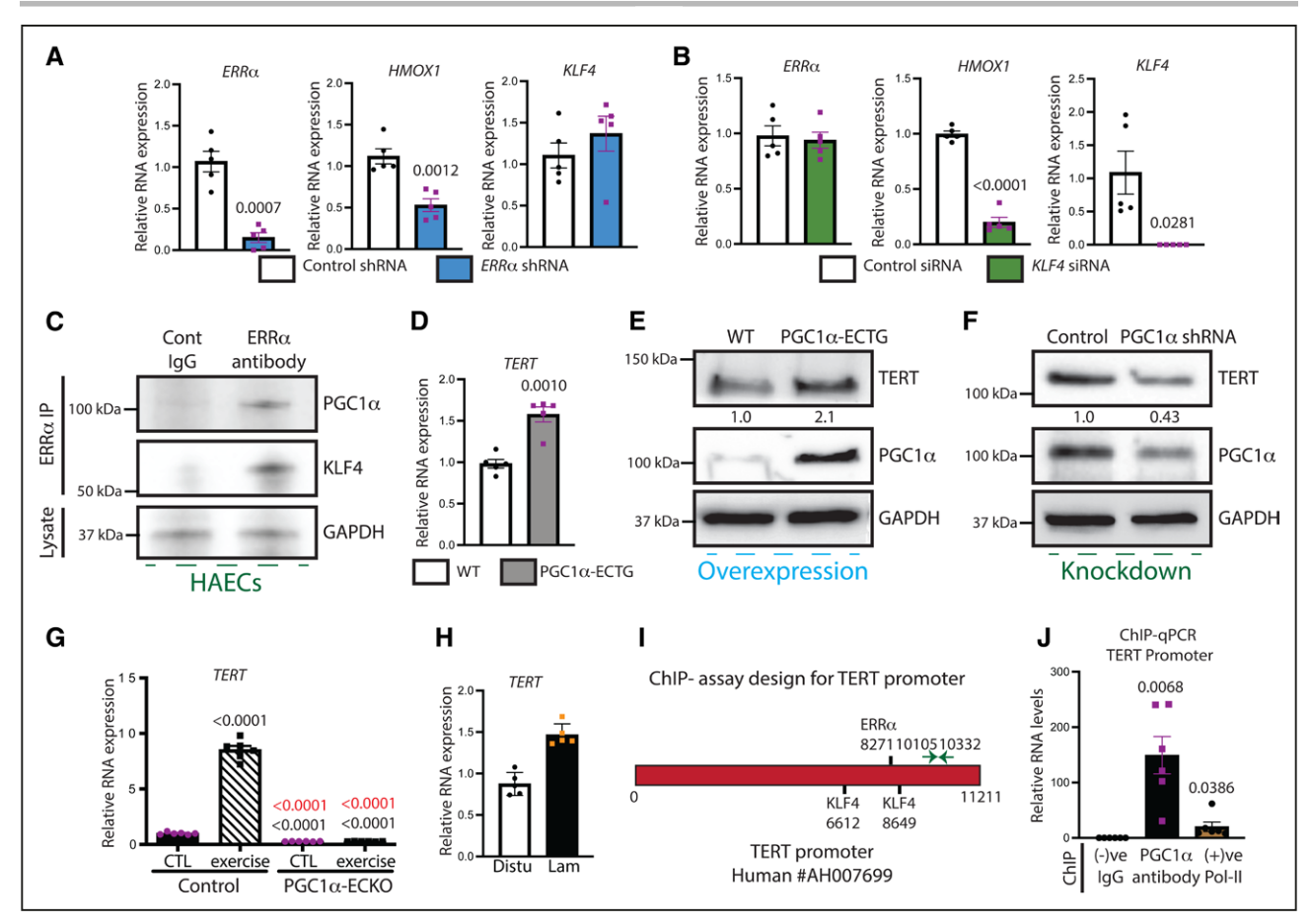


Figure 3. PGC1α (peroxisome proliferator gamma coactivator-1α) regulates TERT (telomerase reverse transcriptase) expression. A and B, Human aortic endothelial cells (HAECs) were either treated with scrambled or *ERR*α (estrogen-related receptor alpha) siRNA (A) or scrambled or *KLF4* siRNA (B), and RT-qPCR (real-time quantitative polymerase chain reaction) was performed for different shear stress-related genes after exposure of cells to laminar fluid shear stress for 48 h (n=5). C, HAECs were lysed, and immunoprecipitation (IP) was performed with control IgG or ERRα antibody, and immunoblotting was done with antibodies against PGC1α and KLF (Kruppel-like factor)-4. Lysates were examined by probing with the GAPDH antibody. D and E, MLECs were isolated from control and PGC1α-ECTG mice, and either RT-qPCR (D) or immunoblot analysis (E) was performed with the probes and antibodies as indicated. F, Lysates prepared from HAECs treated with control shRNA or shRNA against *PGC1α* (48 h) were examined by immunoblot analysis using antibodies for TERT, PGC1α and GAPDH. G, MLECs were isolated from WT (wild type) and PGC1α-ECKO mice, and mRNA expression was measured by RT-qPCR for *TERT* gene before and after exercise (n=6). H, Aortae were isolated, and mRNA expression was measured for TERT by RT-qPCR in the arch and thoracic region of WT mice (n=5). I and J, ChIP (chromatin immunoprecipitation)-qPCR analysis of PGC1α recruitment to the TERT promoter region was performed in HAECs (n=5). All the experiments were repeated 3 to 6 times. Statistically significant differences between groups are indicated. Statistically significant differences were measured by Student *t* test or 1-way ANOVA with post hoc comparison as appropriate with control group. *P* vs control group (black) + exercise group (red) by Student *t* test. The data are mean±SEM.

paraformaldehyde, 7.5% sucrose, and 0.5 mmol/L EDTA, in PBS; and (3) 0.5 mmol/L EDTA in PBS, respectively. Dissected aortae were fixed in 4% paraformaldehyde for 30 minutes and then permeablized with 0.1% Triton X-100 in PBS at room temperature, followed by an overnight incubation (4°C) with a rabbit anti-β-Catenin antibody (Sigma #C2206) in 1:1000 diluted blocking solution (K800621; Dako-Agilent, Carpinteria, CA). Secondary anti-rabbit IgG antibody conjugated with Alexa Plus 555 (Thermo #14-387-071, Waltham, MA) at 1:1500 dilution was used for visualization of endothelial borders. Nuclei were counter stained with 1 µg/mL Hoechst 33342 (Cell Signaling #4082). Vessels were mounted on a coverslip with ProLong anti-fade mounting medium (Thermo #P36962, Waltham, MA). Images were acquired with confocal microscope (Carl Zeiss) and ZEN 2012 software (Carl Zeiss). Since our cell culture work revealed no impact of sex, composite data from en face

staining were typically sampled 4 to $8\times$ in aortae isolated from 4 to 5 mice of either sex. Representative staining in Figure 1 was derived from a male mouse and that in Figure 5 represents a female mouse.

 $PGC1\alpha$ in Fluid Shear Stress

Endothelial Shear Stress Exposure In Vitro

In vitro endothelial cell fluid flow experiments were conducted using either the Ibidi system or a parallel plate flow chamber system as described previously. The Ibidi system used confluent endothelial cells seeded in 0.2% gelatin-coated $\mu\text{-Slide I}$ Luer chambers (Ibidi #80176). Fluid flow conditions involved either unidirectional steady flow (12 dyn/cm²) or bidirectional oscillatory flow (±4 dyn/cm²) using the Ibidi Pump System (Ibidi #10902) for 48-hour treatment. The second system used a parallel plate flow chamber with a peristaltic pump that

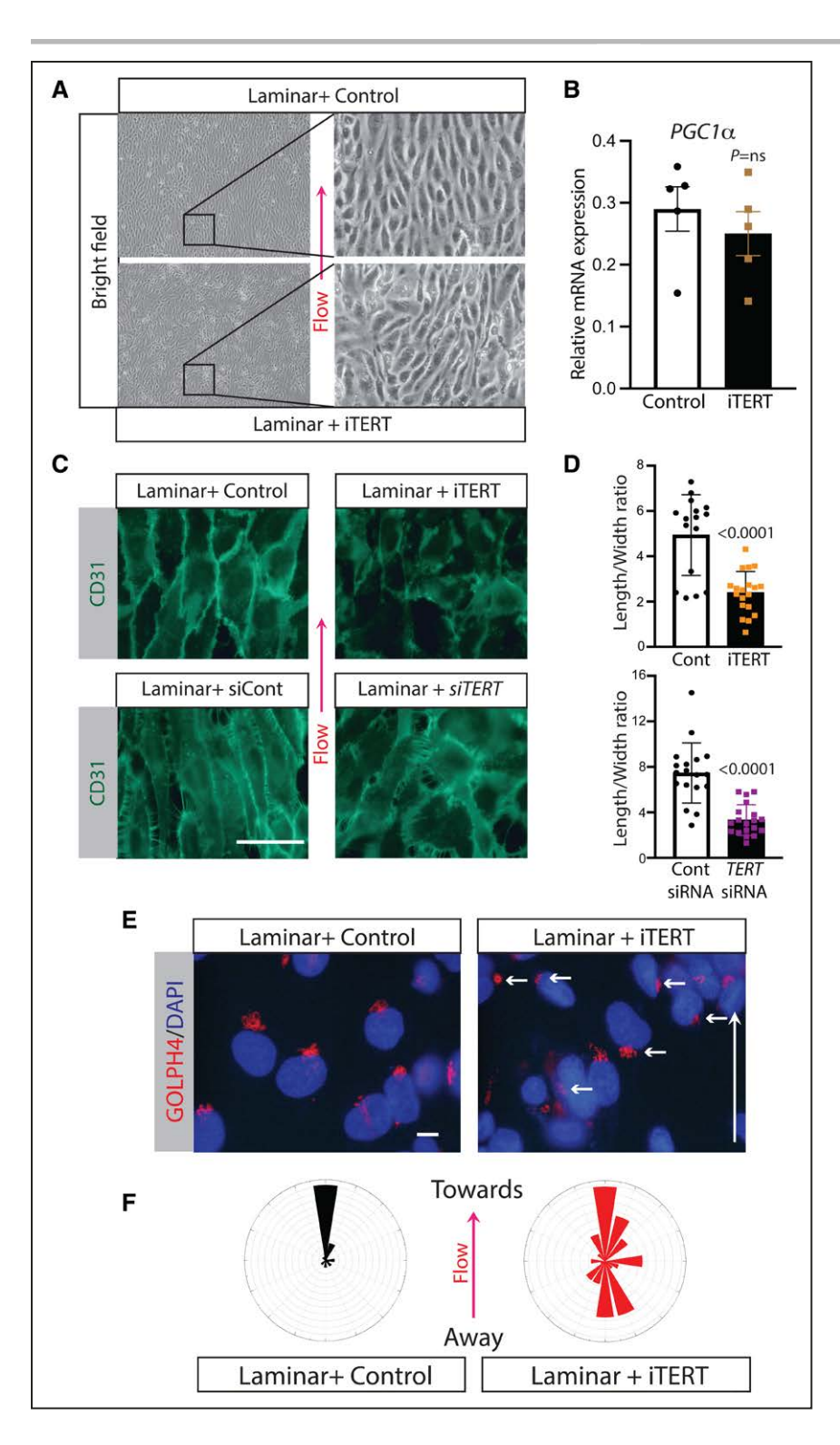


Figure 4. TERT (telomerase reverse transcriptase) is required for endothelial alignment to the flow.

PGC1 α in Fluid Shear Stress

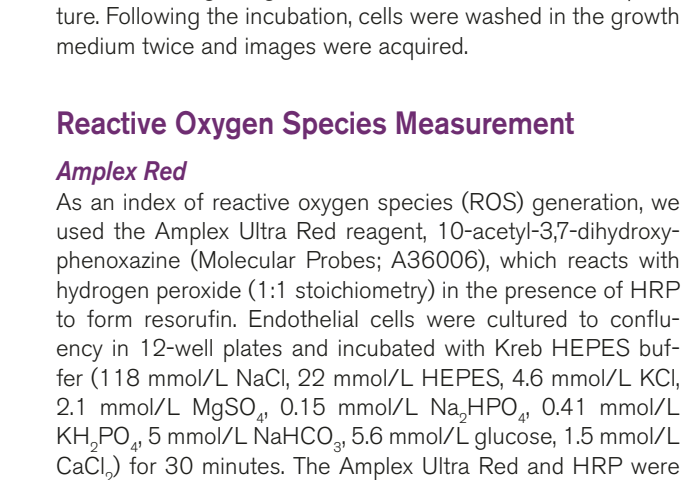
A, Bright-field image of human aortic endothelial cells (HAECs) after exposure to laminar fluid shear stress (FSS) in the presence of either control or TERT inhibitor. B, mRNA was isolated, and $PGC1\alpha$ expression for cells treated with the vehicle control or TERT inhibitor was measured by RT-qPCR (real-time quantitative polymerase chain reaction; n=6). **C**, HAEC morphology was measured by staining for CD31 (cluster of differentiation 31)/DAPI as a function of pharmacological (iTERT) or genetic (siTERT) inhibition of TERT (scale bar, 25 µm). **D**, Length-to-width ratio of CD31 stain in HAECs was measured after TERT inhibition in the presence of laminar FSS (n=15-19), E. HAEC nuclear polarization toward the direction of laminar flow was measured with GOLPH4 (Golgi) and DAPI (nuclei) staining with and without the TERT inhibitor (scale bar, 10 µm). F, Compass plots of Golgi/nuclear angle as a function of TERT inhibition. Each ring represents an observation of an average of different fields of control or TERT inhibitor-treated cells. All the experiments were repeated 3 to 6x. Statistically significant differences between groups are indicated (P vs control by Student ttest). The data are mean±SEM.

generates fully antegrade pulsatile flow (maximum, minimum, and mean wall shear stress equal 6.7, 2.7, and 4.8 dyn/cm², respectively) or net antegrade flow with a flow reversal component (maximum, minimum, and mean wall shear stress equal 1.6, -1.1, and 0.3 dyn/cm², respectively). The steady flow and the fully antegrade pulsatile flow waveforms are referred to as undisturbed flow since the flow is unidirectional. The bidirectional oscillatory flow and the net antegrade flow with a flow reversal component waveform are referred to as disturbed flow

because of the multidirectional nature of the waveforms. The fluidic units were maintained in 37 °C incubators with 5% CO₀.

MitoTracker Staining

Mitochondria in live cells were stained with either MitoTracker obtained from ThermoFisher (MitoTracker Red, M7512, Carlsbad, CA) or CytoPainter MitoRed from Abcam (#ab176832, Cambridge, MA) according to the manufacturer's



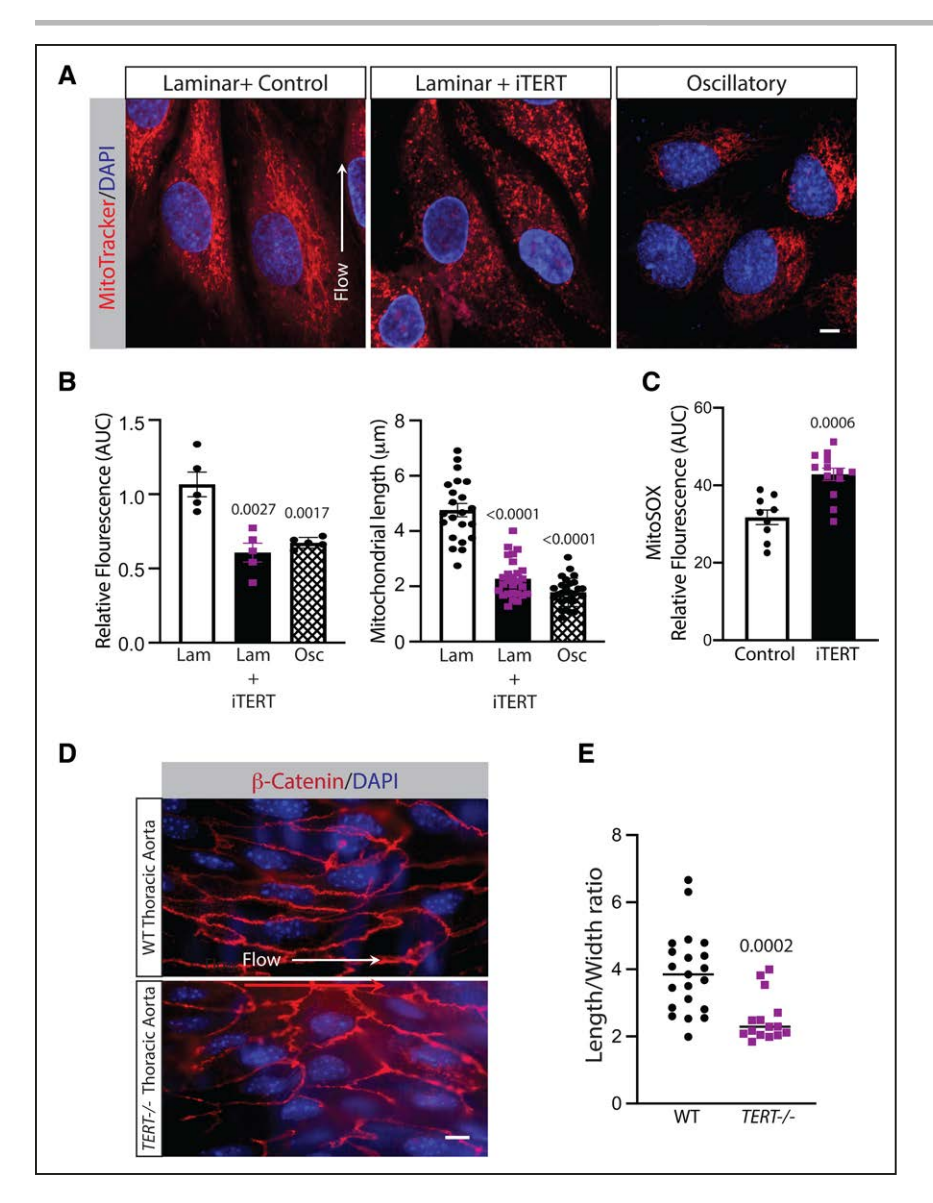


Figure 5. TERT (telomerase reverse transcriptase) regulates mitochondrial structure and function.

A, Mitochondrial morphology and mass (MitoTracker fluorescence) were measured in the presence of laminar flow with and without TERT inhibition (iTERT-BIBR1532) and compared with oscillatory flow (scale bar, 5 µm). B, Quantification of mitochondrial mass (n=5) and morphology during fluid shear stress (n=22-25). C, reactive oxygen species production in human aortic endothelial cells either treated with control or TERT inhibitor (n=9-13). **D**, En face staining with β -Catenin and Hoechst 33342 in WT (wild type) and TERT knockout aorta (scale bar, 10 µm). E, Composite data of length/width ratio of the endothelium in WT and TERT knockout aortae. n is as indicated in each group. All experiments were repeated 3 to 6x. Statistically significant differences were measured by Student t test or 1-way ANOVA with post hoc comparison as appropriate with the control group. The data are mean±SEM.

instructions. In brief, the cells were incubated with 1:1000 diluted MitoTracker/MitoRed in a growth medium for 15 minutes at 37°C incubator and followed by 1 µg/mL Hoechst 33342 (Cell Signaling #4082) for 5 minutes at room tempera-

As an index of reactive oxygen species (ROS) generation, we used the Amplex Ultra Red reagent, 10-acetyl-3,7-dihydroxyphenoxazine (Molecular Probes; A36006), which reacts with hydrogen peroxide (1:1 stoichiometry) in the presence of HRP to form resorufin. Endothelial cells were cultured to confluency in 12-well plates and incubated with Kreb HEPES buffer (118 mmol/L NaCl, 22 mmol/L HEPES, 4.6 mmol/L KCl, 2.1 mmol/L MgSO₄, 0.15 mmol/L Na₃HPO₄, 0.41 mmol/L KH₉PO₄, 5 mmol/L NaHCO₃, 5.6 mmol/L glucose, 1.5 mmol/L CaCl_a) for 30 minutes. The Amplex Ultra Red and HRP were then added, and fluorescence (excitation, 544 nm; emission,

590 nm) was determined as a function of time (2 hours) in 96-well black plates (Corning) at 37°C using a fluorescent plate reader (Spectramax, Molecular Devices). Vascular hydrogen peroxide formation in aortic tissue was measured by an HPLC-based Amplex Red assay as described earlier using aortic ring segments (3 mm in length).32

MitoSOX Red and Dihydroethidium

Total cellular ROS and mitochondrial ROS levels were examined using dihydroethidium and MitoSOX Red, respectively, according to the manufacturer's instructions. Cells were briefly washed and loaded with dihydroethidium (10 µmol/L) or MitoSOX Red (5 μ mol/L) at 37 °C for 20 minutes in the dark and washed 3× with warm buffer. Preloaded cells were incubated at room temperature, 37 °C, 40 °C, or 42 °C for 1, 2, or 3 hours, respectively. To analyze topographical ROS production in aortic tissue, aortic cryosections were used as described previously.33,34

Immunofluorescent Staining

Cells were grown on #1 thick cover glass (EMS #72290-09, Hatfield, PA) or in flow chambers. Cells were fixed with 2% PFA

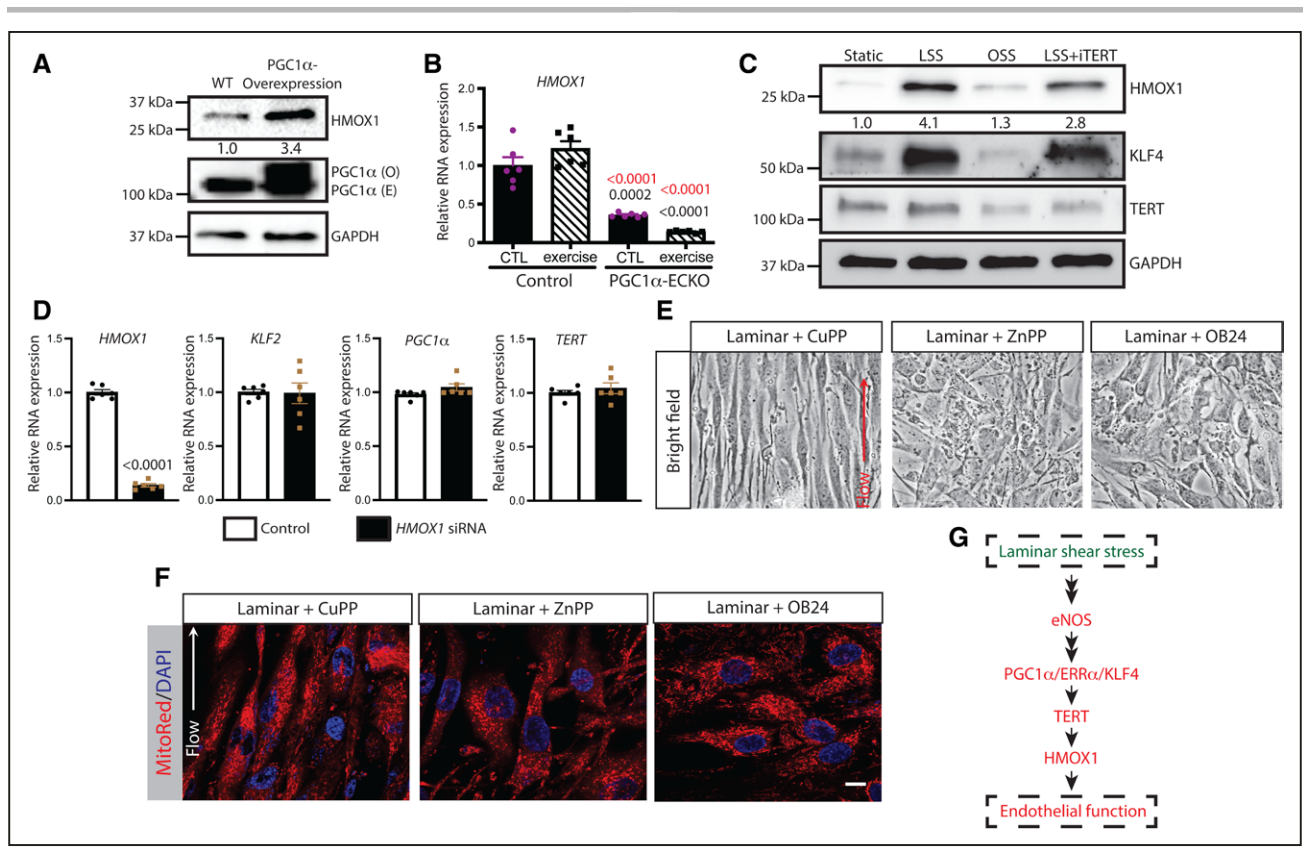


Figure 6. PGC1 α (peroxisome proliferator gamma coactivator-1 α)-TERT (telomerase reverse transcriptase) regulates HMOX1 expression.

A, Mouse lung endothelial cells (MLECs) were isolated from control and PGC1α-ECTG mice, and immunoblot analysis was performed with the antibodies as indicated. B, MLECs were isolated from WT (wild type) and PGC1α-ECKO mice aortae, and mRNA expression was measured by RT-qPCR (real-time quantitative polymerase chain reaction) for the *HMOX1* gene before and after exercise (n=6). C, HAECs (human aortic endothelial cells) were exposed to laminar or oscillatory fluid shear stress (FSS) with or without the TERT inhibitor, and immunoblot analysis was performed with the antibodies as indicated. D, HAECs were either treated with scrambled or *HMOX1* siRNA, and RT-qPCR was performed for different genes related to endothelial function after exposure to laminar FSS for 48 h (n=6). E, Bright-field image of HAECs after exposure to laminar FSS in the presence of either control (copper protoporphyrin IX [CuPP], 0.25 μM) or two different HMOX1 inhibitors (ZnPP, 0.25 μM and OB 24 hydrochloride, 0.25 μM). F, Cell and mitochondrial morphology (MitoRed fluorescence) were imaged in the presence of laminar flow with and without HMOX1 inhibition (Scale bar, 5 μm). G, Schematic diagram of LSS-induced PGC1α-TERT-HMOX1 pathway. n=6 in each group. All the experiments were repeated 3 to 5×. Statistically significant differences between groups are indicated. Statistically significant differences were measured by Student *t* test or 1-way ANOVA with post hoc comparison as appropriate with the control group. *P* vs control group (black)+exercise group (red) by Student *t* test. The data are mean±SEM.

or methanol for 10 minutes followed by permeabilization with 0.1% Triton X-100 (Sigma Aldrich #X100) in PBS. Fixed cells were blocked in blocking solution (K800621; Dako-Agilent), and primary antibodies were incubated at 1:1000 dilution overnight at 4°C. The primary antibodies used were GOLPH4 #ab28049, HMOX1 #ab52947, and TERT #ab32020 (Abcam, Cambridge, MA). Immunocomplexes were visualized with antirabbit secondary antibody conjugated with Alexa Plus 555 (Thermo #14-387-071) or Alexa Plus 488 (Thermo A11034) at 1:1500 dilution. Slides were mounted with an anti-fade mounting medium (Vector Laboratories, Burlingame, CA) containing DAPI and imaged at the Microscopy Resources On the North Quad (MicRoN) facility at the Harvard Medical School, Boston.

Image Analysis

The ImageJ processing software (National Institute of Mental Health, Bethesda, MD) was used to import fluorescent images and separate individual color channels. All area and intensity

values were measured from the green channel. Under digital magnification, the width and height of each hyperfluorescent vessel were manually outlined and the encompassed measurement in pixels converted to micrometer using the scale bar. The average width/height ratio of experimental vessels was compared with the control vessels. For cell polarization, the locations of the nucleus and Golgi were identified, and the angle between the two points relative to the direction of flow was quantified. Three fields were used for quantification from each condition of the experiments. The wind rose plots were compiled using the Origin software (OriginLab 2019, Northampton, MA).

Isometric Measurements of Aortic Function

Thoracic aortic rings (2 mm in length) were mounted on 200 μ M pins in a 6-mL vessel myograph (Danish Myo Technology) containing physiological salt solution consisting of 130 mmol/L NaCl, 4.7 mmol/L KCl, 1.18 mmol/L KHPO₄, 1.17 mmol/L MgSO₄, 1.6 mmol/L CaCl₂, 14.9 mmol/L NaHCO₃, 5.5 mmol/L dextrose,

and 0.03 mmol/L CaNa_o/EDTA. Vessels were stretched to 1 g basal tension at 37°C and aerated with 95% O₂ and 5% CO₂. Vessels were equilibrated in physiological salt solution for 1 hour, followed by 2 consecutive contractions with physiological salt solution containing 60 mmol/L potassium and 1 µM phenylephrine and then with KPSS (high potassium physiological saline solution) alone. Rings were then washed, allowed to return to basal tension, and subjected to concentration-response curves to increasing concentrations of phenylephrine, acetylcholine, and nitroglycerin. Percentage of relaxation was calculated in reference to the degree of phenylephrine precontraction.

Telomerase Length

Telomere length was analyzed using a quantitative polymerase chain reaction (RT-qPCR)-based method described previously.35,36 The relative telomere length was calculated as the ratio of telomere repeats to a single-copy gene (SCG). The acidic ribosomal phosphoprotein PO (36B4) gene was used as the SCG. All qPCRs were performed in duplicates. The primers used for the telomere and the SCG amplification were as follows: telomere forward: 5' GGT TTT TGA GGG TGA GGG TGA GGG TGA GGG TGA GGG T and telomere reverse: 5' TCC CGA CTA TCC CTA TCC CTA TCC CTA TCC CTA; SCG forward: 5' CAG CAA GTG GGA AGG TGT AAT CC and SCG reverse: 5' CCC ATT CTA TCA TCA ACG GGT ACA A.

MLEC Transfection

PGC1α-ECKO MLECs were transfected using either pcDNA3 (Invitrogen, V790-20) or pBABEhygroHigheGFPhTERT (Addgene, 28169) plasmids with DharmaFECT 3 reagent for 6 hours in OptiMEM. MLECs were then changed to growth media containing a 1:1 mixture of DMEM and Ham's F-12 (Gibco), 10% fetal bovine serum, 100 units/mL penicillin, and 100 µg/ mL streptomycin. After 48 hours of plasmid transfection, cells were exposed to laminar flow 12 dynes/cm² (Ibidi System) for 48 hours. Wild-type MLECs were used as a control.

Statistical Analysis

All data are expressed as mean±SEM, and the numbers of independent experiments are indicated. Our analysis strategy involved first testing equal variance and normality of data to determine whether parametric or nonparametric tests were to be used. This strategy lead us to statistical comparisons between 2 groups by use of the parametric Student t test and multiple groups using 1- or 2-way ANOVA with a post hoc Tukey-Kramer multiple comparison as indicated in legends. A P is provided up to 3 decimal digits in figures. All statistics were done using StatView, version 5.0 (SAS Institute, Cary, NC) or GraphPad Prism, version 9 (GraphPad Software, La Jolla, CA).

RESULTS

PGC1α Is Needed for Endothelial Cell Response to FSS

Endothelial cell alignment in the direction of flow involves nuclear polarization and elongation in response to physiological levels of FSS.6 We examined the response of HAECs to oscillatory versus laminar FSS (disturbed versus

undisturbed flow). As expected, oscillatory FSS yielded random HAEC orientation, whereas laminar FSS produced HAEC alignment in the direction of flow (Figure S1A and S1B). Laminar FSS also led to increased expression of key flow-responsive genes, including KLF2,18 KLF4,19,37 HMOX1,38 and HEY139 in both HAECs and human umbilical vein endothelial cells (Figure S1C and S1D). Since PGC1 α has implications for endothelial function, ^{21,40} we examined its expression as a function of FSS. We found that PGC1α mRNA and protein levels were significantly higher with laminar shear stress compared with static control in the human endothelium (Figure 1A and 1B). Similarly, PGC1α mRNA was upregulated with laminar compared with oscillatory flow in 2 different human endothelial cell types (Figures 1B and 2). These data suggest that PGC1 α may play an important role during physiological FSS.

To determine the direct roles of PGC1 α , we utilized lossand gain-of-function strategies. We isolated MLECs from WT mice or endothelial cell-specific PGC1 α knockout (PGC1α-ECKO) mice. Wild-type MLECs subjected to laminar FSS for 48 hours exhibited flow alignment, whereas PGC1αECKO MLECs did not (Figure 1C). Next, a gainof-function strategy was used with MLECs from mice with endothelial-specific PGC1α overexpressing transgenic mice (PGC1α-ECTG) that exhibit ≈60% increase in endothelial PGC1 α compared with WT MLECs.²¹ We found that the static PGC1α-ECTG MLECs exhibited upregulation of the flow-responsive genes KLF48,19 and HMOX138 compared with wild-type cells (Figure 1D). Moreover, PGC1 α -ECTG endothelium demonstrated suppressed ICAM1 and VCAM1 mRNA expression (Figure 1D) compared with wild-type endothelium. Conversely, HAECs with PGC1lphasuppression by siRNA displayed blunted upregulation of HMOX1 and KLF218 in response to laminar FSS compared with the scrambled siRNA control (Figure 1E).

To determine the impact of PGC1 α in vivo, we harvested intact aortic segments from areas of disturbed (inner arch) and laminar (descending thoracic) flow as in Figure 1H. We observed relatively greater PGC1 α mRNA expression in the laminar flow segments compared with areas of disturbed flow (Figure 1F and 1G). Similarly, mRNA expression of HMOX1, KLF2, and KLF4 was upregulated in the laminar versus disturbed flow regions of the aorta in WT and PGC1α-ECTG mice (Figure 1F and 1G). Western blot analysis of aortic segments from areas of disturbed and laminar flow indicated that PGC1 α and HMOX1 protein expression in both WT and PGC1α-ECTG mice was significantly upregulated in laminar flow areas of the aorta compared with areas of disturbed flow (Figure S3A and S3B). We also isolated endothelium from disturbed and laminar flow aortic segments in WT mice and found that endothelial PGC1 α and HMOX1 gene expression were significantly upregulated in laminar versus disturbed flow segments (Figure S3C).

We used en face staining of the aorta with the endothelial junction marker, β-catenin, to assess morphological Kant et al $PGC1\alpha$ in Fluid Shear Stress

endothelial responses to FSS. Endothelial cells adapt to laminar FSS by exhibiting planar cell polarity in the direction of flow. 41,42 The endothelial length-to-width ratio is a key index of flow alignment and planar cell polarity.⁴³ Qualitative assessment of en face staining demonstrated a highly elongated polygon endothelial cell shape and orientation to the vessel's axis in the descending aorta of WT mice (Figure 1I and 1J). Conversely, we observed a reduced endothelial length-to-width ratio in PGC1 α -ECKO descending aorta compared with WT littermate controls (Figure 11 and 1J). Collectively, these data suggest that PGC1 α is a key element of the endothelial morphological and genetic response to FSS.

Endothelial PGC1 α Is Required for the **Endothelial Response to Exercise**

Prolonged exercise is known to increase vascular FSS into the high physiological range and is associated with the upregulation of key FSS-responsive genes that include NOS3, KLF2/4, and HMOX1.44-46 In WT mice subjected to chronic exercise, PGC1 α mRNA expression in the aorta (Figure 2A) and lung endothelium (Figure 2C) was significantly greater than sedentary animals. We also observed that *HMOX1*, as well as *TERT*, a gene sensitive to PGC1 α status in vascular smooth muscle,47 was upregulated in WT mice with chronic exercise but not in PGC1 α -ECKO mice (Figure 2A). Since PGC1 α contributes to ROS detoxification,48 we examined ambient vascular ROS as a function of exercise. Superoxide, mitochondrial ROS and H_oO_o were estimated by dihydroethidium, MitoSOX, and Amplex Red, respectively. We found that chronic exercise reduced all three indices of ROS in WT mice; however, this effect was lost in PGC1 α -ECKO animals (Figure 2B). Endothelial function determined as aortic relaxation to acetylcholine improved with chronic exercise (Figure 2D) in control mice, but this effect was lost in PGC1 α -ECKO animals. Endothelial independent relaxation (using nitroglycerin) was unchanged (Figure 2E), suggesting that the beneficial effect of exercise requires the presence of PGC1 α specifically in vascular endothelium and not smooth muscle (Figure 2D and 2E). These data imply that PGC1 α is an important component of endothelial function during exercise and is required for full exercise-induced HMOX1 and TERT upregulation.

eNOS Controls PGC1α, TERT, and HMOX1 **Expression During FSS**

Laminar flow can induce eNOS (NOS3) activation and NO production in the endothelium.⁴⁹⁻⁵¹ This shear stress activates eNOS, which can lead to endothelial protection by triggering a large number of molecular protective intracellular pathways. 49-51 In addition, NO is well known to activate TERT expression and activity,52 as well as PGC1 α expression.⁵³ Therefore, we examined the roles

of eNOS in PGC1α, TERT, and HMOX1 expression during FSS using eNOS shRNA in HAECs during FSS. Our data showed that eNOS is required for FSS-mediated PGC1α, TERT, and HMOX1 expression in human endothelium (Figure S4).

PGC1α Impacts FSS-Dependent HMOX1 Expression via ERRα and KLF4

 $PGC1\alpha$ impacts gene expression by the coactivation of transcription factors. 54 The transcription factors ERRlphaand KLF4 play a critical role in regulating endothelial function.^{21,55} In cardiac myocytes, ERRα and KLF4 interact with each other and can form a complex with the PGC1 α protein.⁵⁶ Therefore, we examined the role of ERR α and KLF4 in PGC1 α -mediated endothelial responses to laminar FSS. First, using siRNA directed against ERR α in HAECs, we observed that ERR α controls endothelial upregulation of HMOX1 mRNA and protein expression in response to laminar FSS (Figure 3A; Figure S5A). Similarly, KLF4 siRNA inhibited HMOX1 mRNA and protein expression in the setting of laminar FSS (Figure 3B; Figure S5B). In contrast, KLF4 and ERR α had no reciprocal effect on the other's expression with laminar FSS (Figure 3A and 3B). As HMOX1 expression depends on both ERRα and KLF4, we tested their interaction in endothelial cells. $ERR\alpha$ immunoprecipitation demonstrated that it exists in a complex with PGC1 α and KLF4 in human endothelial cells (Figure 3C). These data suggest that ERRa with KLF4 play an important role in PGC1 α -regulated HMOX1 regulation.

PGC1α Dictates TERT Expression in the **Endothelium**

One identified PGC1 α -dependent gene is TERT that, along with TERC, forms the telomerase complex that has been implicated in vascular aging.⁴⁷ In cultured endothelial cells, oxidative stress stimulates nuclear export of TERT to the mitochondria as a protective mechanism,57 and inhibition of telomerase impairs flow-mediated NO bioactivity in human arterioles.58 However, the role of TERT in endothelial responses to FSS is incompletely understood. Therefore, we used PGC1 α gain and loss of function to examine its implications for TERT in FSS responses. We found that PGC1α-ECTG MLECs exhibited upregulation of TERT mRNA and protein (Figure 3D and 3E), whereas PGC1 α shRNA impaired endothelial TERT protein expression (Figure 3F). Also, we examined TERT expression as a function of FSS. Similar to the aortic PGC1 α (Figure 2A), exercise-induced FSS upregulated TERT mRNA in both aorta and MLECs isolated from WT mice but not in PGC1 α -ECKO mice (Figure 2A and 3G). Furthermore, we found that similar to PGC1 α , TERT expression is higher in the laminar flow (thoracic) region of the aorta than in the disturbed flow (inner arch) region (Figure 3H).

Downloaded from http://ahajournals.org by on July 14, 2022

To determine how PGC1 α controls the expression of TERT mRNA, we performed a chromatin immunoprecipitation assay for the human TERT promoter (GenBank# AH007699), which has 2 potential binding sites for KLF4 (Figure 3I; position 6612bp, 8649bp) and 1 for ERRα (Figure 3I; 8271bp). Chromatin immunoprecipitation of the human TERT promoter with the PGC1 α antibody indicated that PGC1 α binds to the TERT promoter region (Figure 3I and 3J). Collectively, these data demonstrate that PGC1 α is required for TERT expression.

TERT Is Required for Endothelial Alignment, **Elongation, and Polarization**

We next examined the impact of TERT on endothelial cell responses to FSS using both pharmacological and molecular approaches. Endothelial cells treated with the TERT inhibitor BIBR1532 (iTERT)⁵⁹ exhibited impaired orientation and alignment in the direction of laminar FSS compared with vehicle-treated cells (Figure 4A). Pharmacological TERT inhibition had no impact on PGC1a expression (Figure 4B). Next, we treated HAECs with siRNA directed against TERT (siTERT) and observed ≈80% reduction in TERT expression levels (Figure S6). Suppression of TERT expression also inhibited HAEC's visual alignment to laminar FSS compared with scrambled siRNA control (Figure 4C). This lack of alignment corresponded to a reduced length-to-width ratio in response to laminar FSS in the presence of either pharmacological or molecular TERT inhibition (Figure 4C and 4D). Another endothelial response to laminar FSS is nuclear polarization with the Golgi directed against the direction of flow.⁶⁰ We examined this phenomenon using the Golgi marker GOLPH4 and found that TERT inhibition prevented nuclear polarization toward laminar flow (Figure 4E and 4F). Collectively, these data show that TERT plays an important role in endothelial cell alignment and polarization in response to laminar FSS.

TERT Is Required for Mitochondrial Responses to FSS

 $PGC1\alpha$ has been known to play an important role in mitochondrial function and biogenesis.61-63 Our data also showed a reduced mitochondrial staining in PGC1 α knockout MLECs compared with WT MLECs (Figure S7). TERT is known to have noncanonical functions that include translocation to the mitochondria and mitochondrial stabilization with oxidative stress.57,64 We probed the implications of TERT in the endothelial FSS response by exposing HAECs to oscillatory versus laminar FSS in the presence or absence of TERT inhibition. We found that laminar FSS produced elongated and branched mitochondrial staining with MitoTracker (Figure 5A). In contrast, TERT inhibition produced punctate mitochondrial morphology that was reminiscent of oscillatory flow (Figure 5A). Composite data

also indicated that TERT inhibition with laminar FSS produces an endothelial response that mimics oscillatory flow with respect to mitochondrial mass by MitoTracker staining and network formation by mitochondrial length (Figure 5B). To determine the role of TERT on mitochondrial ROS, we stained laminar FSS exposed HAECs with MitoSOX as a function of TERT inhibition. Compared with vehicle-treated cells, TERT inhibition enhanced the mitochondrial ROS signal (Figure 5C). Next, we performed immunostaining for TERT and the mitochondria marker CoxIV (cytochrome c oxidase IV). We found that during FSS, TERT colocalizes with the mitochondria in endothelial cells (Figure S8).

TERT has been implicated in telomere length maintenance. Although our experiments were short term, we examined telomere length over the time course of our experiment and found that none of the conditions used for TERT inhibition had any impact on telomere length (Figure S9). These data imply that TERT plays an important role in the endothelial mitochondrial response to laminar FSS that is independent of its canonical function on telomere length. To determine whether these findings play a role in vivo, we used TERT knockout mice. En face staining of endothelial borders with β-catenin in laminar flow segments revealed qualitatively impaired flow alignment in TERT knockout versus wild-type mice (Figure 5D). Composite data of the length:width ratio revealed significantly reduced endothelial elongation in TERT knockout aorta (Figure 5E). These data strongly suggest that TERT is required for optimal endothelial response to laminar FSS in vivo.

TERT Is Required for Normal Laminar FSS-Induced HMOX1 Expression

Our data showed that similar to the KLF4, HMOX1 was also upregulated with laminar FSS (Figure S1). Since our data indicated that both PGC1 α (Figure 1E) and ERR α (Figure 3A) participate in laminar FSS-induced HMOX1 expression, we tested the role of PGC1 α , ERR α , and TERT in this process. First we looked at the expression of HMOX1 in our PGC1 α overexpressing transgenic mice. Endothelial overexpression of PGC1 α increased HMOX1 protein expression under static conditions (Figure 6A), whereas siRNA against ERRα attenuated HMOX1 protein expression during laminar flow (Figure S5A).

Consistent with these findings, exercise-induced FSS upregulated HMOX1 expression in the aorta, as well as in MLECs isolated from exercised mice in a PGC1αdependent manner (Figures 2A and 6B). In terms of TERT, we observed that laminar FSS upregulated HMOX1 protein compared with oscillatory FSS (Figure 6C). Furthermore, our data showed that this upregulation of HMOX1 during laminar flow was dependent upon TERT activity as it was inhibited by a TERT-specific inhibitor, BIBR1532 (Figure 6C). HMOX1 expression appears to be downstream of PGC1\alpha/TERT/KLF2 as HMOX1directed shRNA had no impact on laminar FSS-mediated

expression of these genes (Figure 6D). Next, we performed immunostaining for HMOX1 with mitochondria. Similar to TERT, we found that during FSS, HMOX1 colocalizes with mitochondria in HAECs (Figure S10).

HMOX1 Is Required for the Endothelial Cell Response to the Laminar Flow

To examine whether HMOX1 dictates endothelial FSS responses, we used a pharmacological approach with 2 structurally distinct HMOX1 inhibitors, zinc (II) protoporphyrin IX and 1-[[2-[2-(4-Bromophenyl)ethyl]-1,3-dioxolan-2-yl]methyl]-1*H*-imidazole hydrochloride (OB 24 hydrochloride)⁶⁵⁻⁶⁷ using copper protoporphyrin IX as a control. Copper protoporphyrin IX is a similar compound to zinc (II) protoporphyrin IX but does not inhibit HMOX1.⁶⁵ Both HMOX1 inhibitors impaired HAEC flow alignment in response to laminar FSS compared with control cells treated with copper protoporphyrin IX (Figure 6E). Similarly, HMOX1 inhibition impaired mitochondrial network formation in response to laminar FSS, leaving HAECs with punctate mitochondria as determined by MitoRed staining (Figure 6F).

TERT Can Rescue the Expression of HMOX1 in PGC1 α Knockout MLECs

Since, both PGC1 α and TERT are required for endothelial alignment with laminar flow (Figures 1 and 4), we sought to understand their effects via complementation studies using PGC1 α -ECKO MLECs expressing either control plasmid or TERT-WT plasmid during FSS. We found that TERT can rescue the expression of the downstream target HMOX1 in PGC1 α -ECKO MLECs during laminar flow (Figure S11).

PGC1α-TERT-HMOX1 Pathway Regulates Endothelial-to-Mesenchymal Transition During FSS

Downloaded from http://ahajournals.org by on July 14, 2022

Exposure to low flow rate or disturbed flow causes induction of endothelial-to-mesenchymal transition, resulting in endothelial dysfunction. 14-16 To determine the role of the PGC1α-TERT-HMOX1 pathway in the endothelialto-mesenchymal transition, we used RT-qPCR for the expression of mesenchymal markers in endothelium isolated from PGC1 α -ECTG mice, as well as HAECs treated with TERT and HMOX1 siRNA. We found that forced overexpression of PGC1 α in MLECs suppresses the mesenchymal markers SM22 α (*TagIn*), Sca1 (*Atxn1*), MMP2, and ICAM1 (Figure S12A). Similarly, mesenchymal markers were upregulated in HAECs treated with TERT siRNA or HMOX1 siRNA when compared with control (Figure S12B and S12C). These data support a cascade pathway, depicted in Figure 6G, whereby $PGC1\alpha/ERR\alpha$ contributes to laminar FSS-induced

TERT expression that is needed for the HMOX1 upregulation required for full endothelial FSS responsiveness.

DISCUSSION

The data presented here indicate that PGC1 α is a key element of the endothelial response to FSS. In the absence of PGC1α, endothelial cells exhibited an impaired ability to align and elongate, as well as upregulate key genes characteristic to the response to laminar FSS. These findings appear relevant in vivo, as aortic segments with laminar FSS exhibited PGC1\alpha upregulation; whereas, animals lacking endothelial PGC1α demonstrated impaired flow alignment in the laminar flow sections of the aorta. Similarly, exerciseinduced FSS was associated with improved aortic endothelial function, antioxidant defenses, and reduced ROS which were all impaired in the absence of endothelial PGC1 α . We found that PGC1 α exerted its influence via a complex, including ERR α and KLF4, that affords PGC1 α binding to the TERT promoter to increase TERT expression. In keeping with these findings, TERT upregulation was required for the action of PGC1 α as TERT loss of function recapitulated the endothelial PGC1 α loss-of-function phenotype, including endothelial elongation, flow alignment, mitochondrial stabilization, and HMOX1 upregulation with laminar FSS. With regard to the latter, we found that HMOX1 loss of function was a key downstream mediator of endothelial PGC1 α as HMOX1 inhibition reproduced the endothelial PGC1 α -null phenotype with regard to including flow alignment, elongation, and mitochondrial stabilization. Taken together, these data identify a PGC1α-TERT-HMOX1 axis as a key element of endothelial cell responses to laminar FSS.

eNOS (*NOS3*) is a key component of endothelial function. It is known that shear stress can upregulate and activate eNOS in the endothelium. $^{49-51,68,69}$ In this study, we have clearly shown that eNOS is a key component for shear-induced PGC1 α -TERT-HMOX1 upregulation in the endothelium. One earlier study has implicated the role of eNOS in TERT regulation. 52 These observations are generally consistent with prior literature that implicated the role of NO, via eNOS, is important for mitochondrial biogenesis 70,71 and, in some instances, PGC1 α activation. 70 Initial reports on the mechanism of this response pointed to NO-mediated cGMP production as a key element. 70 However, most prior studies investigated eNOS-mediated control of mitochondria in nonendothelial tissues. Whether or not similar mechanisms apply to the endothelial cell per se are not yet clear.

In response to laminar FSS, we found that upregulation of TERT was required for endothelial elongation, flow alignment, and nuclear polarization. These observations identify TERT as another FSS-sensitive factor that dictates, in part, the endothelial phenotype in response to FSS. The classical function of TERT is restricted to the telomerase complex that prevents cellular senescence typical of aging, particularly in highly replicating tissues.⁷² However, we found no change in endothelial telomere length over the

time course of our study, suggesting that the role of TERT in FSS is independent of its nuclear telomerase function. This contention is supported by studies identifying noncanonical functions of TERT in more quiescent tissues. For example, mice lacking TERT exhibit profound repression of PGC1 α expression in the liver, that mediates impaired mitochondrial biogenesis and function, including gluconeogenesis.73 Endothelial TERT undergoes nuclear export in response to oxidative stress74 and localizes in mitochondria to protect the mitochondrial DNA $^{57,\!64}$ This latter effect may be a consequence of its reverse transcriptase activity toward mitochondrial RNAs.75 More recently, TERT has been implicated in the switch between NO-mediated and ROS-mediated vasodilation in the human microcirculation^{58,76} characteristic of both aging and coronary disease. Whether the functions of TERT in our system are related to its nuclear or mitochondrial localization is not yet clear and will require further study. One might speculate the latter seems plausible since we found TERT was required for the endothelial mitochondrial responses to laminar FSS.

Our study identified TERT upregulation as a key component for the upregulation of HMOX1 with laminar FSS. This is a novel observation that adds to the longstanding knowledge that laminar FSS upregulates HMOX1 and other genes under the control of the ARE (antioxidant response element)77 via activation of the NRF2 (nuclear factor erythroid 2 [NF-E2]-related factor 2)-Keap1 (Kelch-like erythroid cell-derived protein with CNC homology [ECH]-associated protein 1) system.⁷⁸ These data align with the prior knowledge that one stabilizing component of laminar flow on the endothelium is the promotion of an antioxidant state and that HMOX1 upregulation is a key element in this process.⁷⁹ Our data prompt new speculation that TERT could be an important component of the overall cellular ARE phase II detoxification responses. This speculation is consistent with prior observations of TERT nuclear export and activation in response to endothelial oxidative stress.80 The precise elements in the NRF2-ARE pathway that are sensitive to TERT-mediated regulation, however, are not yet clear, although cooperativity between KLF2 and NRF2 has been described in the endothelium.81

An important element of our study is the observation that HMOX1 upregulation is key to endothelial flow alignment and elongation in response to laminar FSS. This is a profound observation in that it adds a completely new consequence of HMOX1 in endothelial cell phenotype. The classic function attributed to HMOX1 is heme degradation, whereas, with laminar FSS, HMOX1 is thought to promote the antioxidant phenotype indicative of quiescent endothelium in atherosclerosis-resistant vascular sites.79 We observed colocalization of TERT control HMOX1 in the endothelium, suggesting some level of cooperativity. Both proteins are known to associate with the nucleus and mitochondria.75,82 Additionally, TERT's association with the latter appears to enhance endothelial resistance to oxidative stress via reverse transcriptase activity.83 HMOX1

localization in the mitochondria is in association with biliverdin reductase and cytochrome P-450 reductase, suggesting its local function is in heme degradation.82 In contrast, HMOX1 nuclear localization has been associated with the upregulation of genes important for oxidative stress.84 Our data indicate that HMOX1 inhibition did not impact the transcription of genes for PGC1α, KLF2, or TERT; however, some transcriptional role of HMOX1 in other laminar FSS-responsive genes cannot yet be ruled out. Nevertheless, our data provide a new role for HMOX1 in the endothelium though the definition of the specific mechanism(s) involved will require further studies.

ARTICLE INFORMATION

Received May 26, 2021; accepted November 2, 2021.

Affiliations

Division of Cardiovascular Medicine, Department of Medicine, Brigham and Women's Hospital, Harvard Medical School, Boston, MA (S.K., A.D.C., H.-J.Y., A.C.D., J.F.K.). Division of Cardiovascular Medicine, Department of Medicine, University of Massachusetts Medical School, Worcester (K.-V.T., H.L.). Department of Cardiology, University Medical Center, Mainz, Germany (M.K., S.K.-S.). Department of Human Nutrition, Foods, and Exercise, Virginia Tech, Blackburg, VA (S.M.C.). Department of Mechanical and Industrial Engineering, University of Massachusetts, Amherst (J.D.H., J.M.J.). Division of Cardiology, Departments of Medicine and Bioengineering, Pittsburgh Heart, Lung, and Blood Vascular Medicine Institute, University of Pittsburgh, PA (C.S.H.). Department of Cardiology, Allgemeines Krankenhaus, Celle, Germany (E.S.).

Acknowledgments

We thank Jennifer Cederberg, Jason Hagan, and Marisol Diaz for academic assistance; Claire C. Chu, Harish Janardhan, and Chinmay Trivedi for technical assistance; and Anastassiia Vertii for critical reading. We would like to thank the Microscopy Resources on the North Quad Core Staff at the Harvard Medical School for their training and support.

Sources of Funding

This work was supported by grant 16SDG29660007 from the American Heart Association (to S. Kant), CAREER CMMI1842308 from the National Science Foundation (to J.M. Jiménez), and K01AR073332 (to S.M. Craige), HL142932 (to C. St. Hilaire), 5T32HL120823 (to K.-V. Tran), 5T32GM135096 (to J.D. Hall), and HL151626 (to J.F. Keaney) from the National Institutes of Health.

Disclosures

None.

Supplemental Material

Figures S1-S12 Supplemental Major Resources Table Footnotes

REFERENCES

- 1. Potente M, Carmeliet P. The link between angiogenesis and endothelial metabolism. Annu Rev Physiol. 2017;79:43-66. doi: 10.1146/annurevphysiol-021115-105134
- 2. Craige SM, Kant S, Keaney JF Jr. Reactive oxygen species in endothelial function - from disease to adaptation -. Circ J. 2015;79:1145-1155. doi: 10.1253/circj.CJ-15-0464
- Widlansky ME, Gokce N, Keaney JF Jr, Vita JA. The clinical implications of endothelial dysfunction. J Am Coll Cardiol. 2003;42:1149-1160. doi: 10.1016/s0735-1097(03)00994-x
- 4. Gimbrone MA Jr, García-Cardeña G. Endothelial cell dysfunction and the pathobiology of atherosclerosis. Circ Res. 2016;118:620-636. doi: 10.1161/ CIRCRESAHA.115.306301
- 5. Baeyens N, Bandyopadhyay C, Coon BG, Yun S, Schwartz MA. Endothelial fluid shear stress sensing in vascular health and disease. J Clin Invest. 2016;126:821-828. doi: 10.1172/JCI83083
- 6. Noria S, Xu F, McCue S, Jones M, Gotlieb Al, Langille BL. Assembly and reorientation of stress fibers drives morphological changes to endothelial

Kant et al

Downloaded from http://ahajournals.org by on July 14, 2022

- cells exposed to shear stress. *Am J Pathol.* 2004;164:1211-1223. doi: 10.1016/S0002-9440(10)63209-9
- Zhou J, Li YS, Chien S. Shear stress-initiated signaling and its regulation of endothelial function. *Arterioscler Thromb Vasc Biol.* 2014;34:2191–2198. doi: 10.1161/ATVBAHA.114.303422
- Davies PF, Civelek M, Fang Y, Fleming I. The atherosusceptible endothelium: endothelial phenotypes in complex haemodynamic shear stress regions in vivo. Cardiovasc Res. 2013;99:315–327. doi: 10.1093/cvr/cvt101
- Baeyens N. Fluid shear stress sensing in vascular homeostasis and remodeling: towards the development of innovative pharmacological approaches to treat vascular dysfunction. *Biochem Pharmacol.* 2018;158:185–191. doi: 10.1016/j.bcp.2018.10.023
- Wang C, Baker BM, Chen CS, Schwartz MA. Endothelial cell sensing of flow direction. Arterioscler Thromb Vasc Biol. 2013;33:2130–2136. doi: 10.1161/ATVBAHA.113.301826
- Peiffer V, Sherwin SJ, Weinberg PD. Computation in the rabbit aorta of a new metric - the transverse wall shear stress - to quantify the multidirectional character of disturbed blood flow. *J Biomech.* 2013;46:2651–2658. doi: 10.1016/j.jbiomech.2013.08.003
- Coon BG, Baeyens N, Han J, Budatha M, Ross TD, Fang JS, Yun S, Thomas JL, Schwartz MA. Intramembrane binding of VE-cadherin to VEGFR2 and VEGFR3 assembles the endothelial mechanosensory complex. J Cell Biol. 2015;208:975–986. doi: 10.1083/jcb.201408103
- Baeyens N, Nicoli S, Coon BG, Ross TD, Van den Dries K, Han J, Lauridsen HM, Mejean CO, Eichmann A, Thomas JL, et al. Vascular remodeling is governed by a VEGFR3-dependent fluid shear stress set point. *Elife*. 2015;4.
- Min E, Schwartz MA. Translocating transcription factors in fluid shear stressmediated vascular remodeling and disease. Exp Cell Res. 2019;376:92–97. doi: 10.1016/j.yexcr.2019.01.005
- Wang L, Luo JY, Li B, Tian XY, Chen LJ, Huang Y, Liu J, Deng D, Lau CW, Wan S, et al. Integrin-YAP/TAZ-JNK cascade mediates atheroprotective effect of unidirectional shear flow. *Nature*. 2016;540:579–582. doi: 10.1038/nature20602
- Poduri A, Chang AH, Raftrey B, Rhee S, Van M, Red-Horse K. Endothelial cells respond to the direction of mechanical stimuli through SMAD signaling to regulate coronary artery size. *Development*. 2017;144:3241–3252. doi: 10.1242/dev.150904
- Doddaballapur A, Michalik KM, Manavski Y, Lucas T, Houtkooper RH, You X, Chen W, Zeiher AM, Potente M, Dimmeler S, et al. Laminar shear stress inhibits endothelial cell metabolism via KLF2-mediated repression of PFKFB3. Arterioscler Thromb Vasc Biol. 2015;35:137–145. doi: 10.1161/ATVBAHA.114.304277
- Huddleson JP, Ahmad N, Srinivasan S, Lingrel JB. Induction of KLF2 by fluid shear stress requires a novel promoter element activated by a phosphatidylinositol 3-kinase-dependent chromatin-remodeling pathway. J Biol Chem. 2005;280:23371–23379. doi: 10.1074/jbc.M413839200
- Sangwung P, Zhou G, Nayak L, Chan ER, Kumar S, Kang DW, Zhang R, Liao X, Lu Y, Sugi K, et al. KLF2 and KLF4 control endothelial identity and vascular integrity. *JCI Insight*. 2017;2:e91700. doi: 10.1172/jci.insight.91700
- Jain MK, Sangwung P, Hamik A. Regulation of an inflammatory disease: Krüppel-like factors and atherosclerosis. Arterioscler Thromb Vasc Biol. 2014;34:499–508. doi: 10.1161/ATVBAHA.113.301925
- Craige SM, Kröller-Schön S, Li C, Kant S, Cai S, Chen K, Contractor MM, Pei Y, Schulz E, Keaney JF Jr. PGC-1α dictates endothelial function through regulation of eNOS expression. Sci Rep. 2016;6:38210. doi: 10.1038/srep38210
- Lin J, Wu PH, Tarr PT, Lindenberg KS, St-Pierre J, Zhang CY, Mootha VK, Jäger S, Vianna CR, Reznick RM, et al. Defects in adaptive energy metabolism with CNS-linked hyperactivity in PGC-1alpha null mice. *Cell*. 2004;119:121–135. doi: 10.1016/j.cell.2004.09.013
- Chiang YJ, Hemann MT, Hathcock KS, Tessarollo L, Feigenbaum L, Hahn WC, Hodes RJ. Expression of telomerase RNA template, but not telomerase reverse transcriptase, is limiting for telomere length maintenance in vivo. *Mol Cell Biol.* 2004;24:7024–7031. doi: 10.1128/MCB. 24.16.7024-7031.2004
- Liu T, Yu H, Ding L, Wu Z, Gonzalez De Los Santos F, Liu J, Ullenbruch M, Hu B, Martins V, Phan SH. Conditional knockout of telomerase reverse transcriptase in mesenchymal cells impairs mouse pulmonary fibrosis. *PLoS One*. 2015;10:e0142547. doi: 10.1371/journal.pone.0142547
- Craige SM, Kant S, Reif M, Chen K, Pei Y, Angoff R, Sugamura K, Fitzgibbons T, Keaney JF Jr. Endothelial NADPH oxidase 4 protects ApoE-/-mice from atherosclerotic lesions. Free Radic Biol Med. 2015;89:1–7. doi: 10.1016/j.freeradbiomed.2015.07.004
- Schreiber SN, Knutti D, Brogli K, Uhlmann T, Kralli A. The transcriptional coactivator PGC-1 regulates the expression and activity of the orphan

nuclear receptor estrogen-related receptor alpha (ERRalpha). J Biol Chem. 2003;278:9013–9018. doi: 10.1074/jbc.M212923200

PGC1α in Fluid Shear Stress

- Kant S, Swat W, Zhang S, Zhang ZY, Neel BG, Flavell RA, Davis RJ. TNFstimulated MAP kinase activation mediated by a Rho family GTPase signaling pathway. *Genes Dev.* 2011;25:2069–2078. doi: 10.1101/gad.17224711
- Livak KJ, Schmittgen TD. Analysis of relative gene expression data using real-time quantitative PCR and the 2(-delta delta C(T)) method. *Methods*. 2001;25:402–408. doi: 10.1006/meth.2001.1262
- Rao X, Huang X, Zhou Z, Lin X. An improvement of the 2⁻(-delta delta CT) method for quantitative real-time polymerase chain reaction data analysis. Biostat Bioinforma Biomath. 2013;3:71–85.
- Caliz AD, Yoo HJ, Vertii A, Dolan AC, Tournier C, Davis RJ, Keaney JF Jr, Kant S. Mitogen Kinase Kinase (MKK7) Controls Cytokine Production In Vitro and In Vivo in Mice. Int J Mol Sci. 2021;22:9364. doi: 10.3390/ijms22179364
- Jiménez JM, Prasad V, Yu MD, Kampmeyer CP, Kaakour AH, Wang PJ, Maloney SF, Wright N, Johnston I, Jiang YZ, et al. Macro- and microscale variables regulate stent haemodynamics, fibrin deposition and thrombomodulin expression. J R Soc Interface. 2014;11:20131079. doi: 10.1098/rsif.2013.1079
- 32. Kröller-Schön S, Steven S, Kossmann S, Scholz A, Daub S, Oelze M, Xia N, Hausding M, Mikhed Y, Zinssius E, et al. Molecular mechanisms of the crosstalk between mitochondria and NADPH oxidase through reactive oxygen species-studies in white blood cells and in animal models. *Antioxid Redox Signal*. 2014;20:247–266. doi: 10.1089/ars.2012.4953
- Chrissobolis S, Drummond GR, Faraci FM, Sobey CG. Chronic aldosterone administration causes Nox2-mediated increases in reactive oxygen species production and endothelial dysfunction in the cerebral circulation. *J Hyper*tens. 2014;32:1815–1821. doi: 10.1097/HJH.0000000000000259
- Hink U, Li H, Mollnau H, Oelze M, Matheis E, Hartmann M, Skatchkov M, Thaiss F, Stahl RA, Warnholtz A, et al. Mechanisms underlying endothelial dysfunction in diabetes mellitus. Circ Res. 2001;88:E14–E22. doi: 10.1161/01.res.88.2.e14
- Dlouha D, Maluskova J, Kralova Lesna I, Lanska V, Hubacek JA. Comparison of the relative telomere length measured in leukocytes and eleven different human tissues. *Physiol Res.* 2014;63(suppl 3):S343–S350. doi: 10.33549/physiolres.932856
- Cawthon RM. Telomere measurement by quantitative PCR. Nucleic Acids Res. 2002;30:e47. doi: 10.1093/nar/30.10.e47
- Hamik A, Lin Z, Kumar A, Balcells M, Sinha S, Katz J, Feinberg MW, Gerzsten RE, Edelman ER, Jain MK. Kruppel-like factor 4 regulates endothelial inflammation. J Biol Chem. 2007;282:13769–13779. doi: 10.1074/jbc.M700078200
- Ali F, Zakkar M, Karu K, Lidington EA, Hamdulay SS, Boyle JJ, Zloh M, Bauer A, Haskard DO, Evans PC, et al. Induction of the cytoprotective enzyme heme oxygenase-1 by statins is enhanced in vascular endothelium exposed to laminar shear stress and impaired by disturbed flow. *J Biol Chem.* 2009;284:18882–18892. doi: 10.1074/jbc.M109.009886
- Wang P, Zhu S, Yuan C, Wang L, Xu J, Liu Z. Shear stress promotes differentiation of stem cells from human exfoliated deciduous teeth into endothelial cells via the downstream pathway of VEGF-Notch signaling. *Int J Mol Med.* 2018;42:1827–1836. doi: 10.3892/ijmm.2018.3761
- Kadlec AO, Chabowski DS, Ait-Aissa K, Gutterman DD. Role of PGC-1α in vascular regulation: implications for atherosclerosis. *Arterioscler Thromb* Vasc Biol. 2016;36:1467–1474. doi: 10.1161/ATVBAHA.116.307123
- McCue S, Dajnowiec D, Xu F, Zhang M, Jackson MR, Langille BL. Shear stress regulates forward and reverse planar cell polarity of vascular endothelium in vivo and in vitro. Circ Res. 2006;98:939–946. doi: 10.1161/01.RES.0000216595.15868.55
- Mack JJ, Mosqueiro TS, Archer BJ, Jones WM, Sunshine H, Faas GC, Briot A, Aragón RL, Su T, Romay MC, et al. NOTCH1 is a mechanosensor in adult arteries. *Nat Commun.* 2017;8:1620. doi: 10.1038/s41467-017-01741-8
- Sumagin R, Brown CW III, Sarelius IH, King MR. Microvascular endothelial cells exhibit optimal aspect ratio for minimizing flow resistance. *Ann Biomed Eng.* 2008;36:580–585. doi: 10.1007/s10439-008-9467-2
- Sessa WC, Pritchard K, Seyedi N, Wang J, Hintze TH. Chronic exercise in dogs increases coronary vascular nitric oxide production and endothelial cell nitric oxide synthase gene expression. *Circ Res.* 1994;74:349–353. doi: 10.1161/01.res.74.2.349
- Di Francescomarino S, Sciartilli A, Di Valerio V, Di Baldassarre A, Gallina S. The effect of physical exercise on endothelial function. Sports Med. 2009;39:797–812. doi: 10.2165/11317750-000000000-00000
- 46. Min SY, Learnard H, Kant S, Gealikman O, Rojas-Rodriguez R, DeSouza T, Desai A, Keaney JF Jr, Corvera S, Craige SM. Exercise rescues gene pathways involved in vascular expansion and promotes functional angiogenesis

- in subcutaneous white adipose tissue. *Int J Mol Sci.* 2019;20:E2046. doi: 10.3390/ijms20082046
- Xiong S, Patrushev N, Forouzandeh F, Hilenski L, Alexander RW. PGC-1α modulates telomere function and DNA damage in protecting against aging-related chronic diseases. *Cell Rep.* 2015;12:1391–1399. doi: 10.1016/j.celrep.2015.07.047
- St-Pierre J, Drori S, Uldry M, Silvaggi JM, Rhee J, Jäger S, Handschin C, Zheng K, Lin J, Yang W, et al. Suppression of reactive oxygen species and neurodegeneration by the PGC-1 transcriptional coactivators. *Cell.* 2006;127:397–408. doi: 10.1016/j.cell.2006.09.024
- Malek AM, Jiang L, Lee I, Sessa WC, Izumo S, Alper SL. Induction of nitric oxide synthase mRNA by shear stress requires intracellular calcium and G-protein signals and is modulated by PI 3 kinase. *Biochem Biophys Res* Commun. 1999;254:231–242. doi: 10.1006/bbrc.1998.9921
- Xiao Z, Zhang Z, Ranjan V, Diamond SL. Shear stress induction of the endothelial nitric oxide synthase gene is calcium-dependent but not calcium-activated. *J Cell Physiol*. 1997;171:205-211.doi:10.1002/(SICI)1097-4652(199705)171:2<205::AID-JCP11>3.0.CO;2-C
- Uematsu M, Ohara Y, Navas JP, Nishida K, Murphy TJ, Alexander RW, Nerem RM, Harrison DG. Regulation of endothelial cell nitric oxide synthase mRNA expression by shear stress. *Am J Physiol.* 1995;269(6 Pt 1):C1371-C1378. doi: 10.1152/ajpcell.1995.269.6.C1371
- Grasselli A, Nanni S, Colussi C, Aiello A, Benvenuti V, Ragone G, Moretti F, Sacchi A, Bacchetti S, Gaetano C, et al. Estrogen receptor-alpha and endothelial nitric oxide synthase nuclear complex regulates transcription of human telomerase. *Circ Res.* 2008;103:34–42. doi: 10.1161/ CIRCRESAHA.107.169037
- Lira VA, Brown DL, Lira AK, Kavazis AN, Soltow OA, Zeanah EH, Criswell DS. Nitric oxide and AMPK cooperatively regulate PGC-1 in skeletal muscle cells. J Physiol. 2010;588(pt 18):3551–3566. doi: 10.1113/ jphysiol.2010.194035
- Finck BN, Kelly DP. PGC-1 coactivators: inducible regulators of energy metabolism in health and disease. J Clin Invest. 2006;116:615–622. doi: 10.1172/JCI27794
- Zhou G, Hamik A, Nayak L, Tian H, Shi H, Lu Y, Sharma N, Liao X, Hale A, Boerboom L, et al. Endothelial Kruppel-like factor 4 protects against atherothrombosis in mice. *J Clin Invest*. 2012;122:4727–4731. doi: 10.1172/JCI66056
- Jang C, Arany Z. Mitochondria Cripple without Krüppel. Trends Endocrinol Metab. 2015;26:587–589. doi: 10.1016/j.tem.2015.08.004
- Haendeler J, Dröse S, Büchner N, Jakob S, Altschmied J, Goy C, Spyridopoulos I, Zeiher AM, Brandt U, Dimmeler S. Mitochondrial telomerase reverse transcriptase binds to and protects mitochondrial DNA and function from damage. *Arterioscler Thromb Vasc Biol.* 2009;29:929–935. doi: 10.1161/ATVBAHA.109.185546
- Beyer AM, Freed JK, Durand MJ, Riedel M, Ait-Aissa K, Green P, Hockenberry JC, Morgan RG, Donato AJ, Peleg R, et al. Critical Role for Telomerase in the Mechanism of Flow-Mediated Dilation in the Human Microcirculation. Circ Res. 2016;118:856–866. doi: 10.1161/CIRCRESAHA. 115.307918
- Bryan C, Rice C, Hoffman H, Harkisheimer M, Sweeney M, Skordalakes E. Structural basis of telomerase inhibition by the highly specific BIBR1532. Structure. 2015;23:1934–1942. doi: 10.1016/j.str.2015.08.006
- Franco CA, Jones ML, Bernabeu MO, Geudens I, Mathivet T, Rosa A, Lopes FM, Lima AP, Ragab A, Collins RT, et al. Dynamic endothelial cell rearrangements drive developmental vessel regression. *PLoS Biol.* 2015;13:e1002125. doi: 10.1371/journal.pbio.1002125
- Cherry AD, Suliman HB, Bartz RR, Piantadosi CA. Peroxisome proliferator-activated receptor γ co-activator 1-α as a critical co-activator of the murine hepatic oxidative stress response and mitochondrial biogenesis in Staphylococcus aureus sepsis. *J Biol Chem.* 2014;289:41-52. doi: 10.1074/jbc.M113.512483
- Gleyzer N, Vercauteren K, Scarpulla RC. Control of mitochondrial transcription specificity factors (TFB1M and TFB2M) by nuclear respiratory factors (NRF-1 and NRF-2) and PGC-1 family coactivators. *Mol Cell Biol.* 2005;25:1354–1366.doi: 10.1128/MCB.25.4.1354-1366.2005
- Singh SP, Schragenheim J, Cao J, Falck JR, Abraham NG, Bellner L. PGC-1 alpha regulates HO-1 expression, mitochondrial dynamics and biogenesis: role of epoxyeicosatrienoic acid. *Prostaglandins Other Lipid Mediat*. 2016;125:8–18. doi: 10.1016/j.prostaglandins.2016.07.004
- 64. Santos JH, Meyer JN, Van Houten B. Mitochondrial localization of telomerase as a determinant for hydrogen peroxide-induced mitochondrial DNA damage and apoptosis. *Hum Mol Genet*. 2006;15:1757–1768. doi: 10.1093/hmg/ddl098

- Tozer GM, Prise VE, Motterlini R, Poole BA, Wilson J, Chaplin DJ. The comparative effects of the NOS inhibitor, nomega-nitro-L-arginine, and the haemoxygenase inhibitor, zinc protoporphyrin IX, on tumour blood flow. Int J Radiat Oncol Biol Phys. 1998;42:849–853. doi: 10.1016/s0360-3016(98)00303-4
- Khelifi AF, Prise VE, Tozer GM. Effects of tin-protoporphyrin IX on blood flow in a rat tumor model. Exp Biol Med (Maywood). 2003;228:481–485. doi: 10.1177/15353702-0322805-10
- 67. Alaoui-Jamali MA, Bismar TA, Gupta A, Szarek WA, Su J, Song W, Xu Y, Xu B, Liu G, Vlahakis JZ, et al. A novel experimental heme oxygenase-1-targeted therapy for hormone-refractory prostate cancer. *Cancer Res.* 2009;69:8017–8024. doi: 10.1158/0008-5472.CAN-09-0419
- Traub O, Berk BC. Laminar shear stress: mechanisms by which endothelial cells transduce an atheroprotective force. *Arterioscler Thromb Vasc Biol.* 1998;18:677–685. doi: 10.1161/01.atv.18.5.677
- Boo YC, Jo H. Flow-dependent regulation of endothelial nitric oxide synthase: role of protein kinases. Am J Physiol Cell Physiol. 2003;285:C499–C508. doi: 10.1152/ajpcell.00122.2003
- Nisoli E, Clementi E, Paolucci C, Cozzi V, Tonello C, Sciorati C, Bracale R, Valerio A, Francolini M, Moncada S, et al. Mitochondrial biogenesis in mammals: the role of endogenous nitric oxide. *Science*. 2003;299:896–899. doi: 10.1126/science.1079368
- Nisoli E, Falcone S, Tonello C, Cozzi V, Palomba L, Fiorani M, Pisconti A, Brunelli S, Cardile A, Francolini M, et al. Mitochondrial biogenesis by NO yields functionally active mitochondria in mammals. *Proc Natl Acad Sci USA*. 2004;101:16507–16512. doi: 10.1073/pnas.0405432101
- Martínez P, Blasco MA. Heart-breaking telomeres. Circ Res. 2018;123:787–802. doi: 10.1161/CIRCRESAHA.118.312202
- Sahin E, Colla S, Liesa M, Moslehi J, Müller FL, Guo M, Cooper M, Kotton D, Fabian AJ, Walkey C, et al. Telomere dysfunction induces metabolic and mitochondrial compromise. *Nature*. 2011;470:359–365. doi: 10.1038/nature09787
- Haendeler J, Hoffmann J, Brandes RP, Zeiher AM, Dimmeler S. Hydrogen peroxide triggers nuclear export of telomerase reverse transcriptase via Src kinase family-dependent phosphorylation of tyrosine 707. Mol Cell Biol. 2003;23:4598–4610. doi: 10.1128/MCB.23.13.4598-4610.2003
- Sharma NK, Reyes A, Green P, Caron MJ, Bonini MG, Gordon DM, Holt IJ, Santos JH. Human telomerase acts as a hTR-independent reverse transcriptase in mitochondria. *Nucleic Acids Res.* 2012;40:712–725. doi: 10.1093/nar/gkr758
- Hughes WE, Chabowski DS, Ait-Aissa K, Fetterman JL, Hockenberry J, Beyer AM, Gutterman DD. Critical interaction between telomerase and autophagy in mediating flow-induced human arteriolar vasodilation. *Arterioscler Thromb Vasc Biol.* 2020;41:446–457. doi: 10.1161/ATVBAHA.120.314944
- Chen XL, Varner SE, Rao AS, Grey JY, Thomas S, Cook CK, Wasserman MA, Medford RM, Jaiswal AK, Kunsch C. Laminar flow induction of antioxidant response element-mediated genes in endothelial cells. A novel anti-inflammatory mechanism. *J Biol Chem.* 2003;278:703–711. doi: 10.1074/jbc.M203161200
- Hosoya T, Maruyama A, Kang MI, Kawatani Y, Shibata T, Uchida K, Warabi E, Noguchi N, Itoh K, Yamamoto M. Differential responses of the Nrf2-Keap1 system to laminar and oscillatory shear stresses in endothelial cells. *J Biol Chem.* 2005;280:27244–27250. doi: 10.1074/jbc.M502551200
- Berk BC. Atheroprotective signaling mechanisms activated by steady laminar flow in endothelial cells. *Circulation*. 2008;117:1082–1089. doi: 10.1161/CIRCULATIONAHA.107.720730
- Haendeler J, Hoffmann J, Diehl JF, Vasa M, Spyridopoulos I, Zeiher AM, Dimmeler S. Antioxidants inhibit nuclear export of telomerase reverse transcriptase and delay replicative senescence of endothelial cells. *Circ Res.* 2004;94:768–775. doi: 10.1161/01.RES.0000121104.05977.F3
- Fledderus JO, Boon RA, Volger OL, Hurttila H, Ylä-Herttuala S, Pannekoek H, Levonen AL, Horrevoets AJ. KLF2 primes the antioxidant transcription factor Nrf2 for activation in endothelial cells. *Arterioscler Thromb Vasc Biol.* 2008;28:1339–1346. doi: 10.1161/ATVBAHA.108.165811
- Dunn LL, Midwinter RG, Ni J, Hamid HA, Parish CR, Stocker R. New insights into intracellular locations and functions of heme oxygenase-1. *Antioxid Redox Signal*. 2014;20:1723–1742. doi: 10.1089/ars.2013.5675
- Rosen J, Jakobs P, Ale-Agha N, Altschmied J, Haendeler J. Non-canonical functions of telomerase reverse transcriptase - impact on redox homeostasis. *Redox Biol.* 2020;34:101543. doi: 10.1016/j.redox.2020.101543
- 84. Lin Q, Weis S, Yang G, Weng YH, Helston R, Rish K, Smith A, Bordner J, Polte T, Gaunitz F, et al. Heme oxygenase-1 protein localizes to the nucleus and activates transcription factors important in oxidative stress. *J Biol Chem.* 2007;282:20621–20633. doi: 10.1074/jbc.M607954200